مركز الأكاديمية للنشر
ACADEMY Publishing Center

RESD
Renewable Energy and Sustainable Development Journal

- ISSN 2356-8569

Volume 8
Issue 2
December
2022

Academy Publishing Center
Journal of Renewable Energy and Sustainable Development (RESD)

RESD
Volume 8, Issue 2, December 2022
p-ISSN: 2356-8518 Print Version
e-ISSN: 2356-8569 Online Version

http://apc.aast.edu

Arab Academy for Science, Technology, and Maritime Transport, AASTMT Abu Kir Campus, Alexandria, EGYPT
P.O. Box: Miami 1029
Tel: (+203) 5622366/88 – EXT 1069 and (+203) 5611818
Fax: (+203) 5611818
Web Site: http://apc.aast.edu

RESD Journal of Renewable Energy and Sustainable Development

Renewable Energy and Sustainable Development (RESD) is a biannual international peer-reviewed journal, which presents a global forum for dissemination of research articles, case studies and reviews focusing on all aspects of renewable energy and its role in sustainable development. The topics of focal interest to RESD include, but are not limited to, all aspects of wind energy, wave/tidal energy, solar energy, as well as energy from biomass and biofuel. The integration of renewable energy technologies in electrical power networks and smart grids is another topic of interest to RESD. Experimental, computational and theoretical studies are all welcomed to RESD.

Sustainable development is a multidisciplinary advancing to the center of energy research with the declaration of UN millennium development goals for the first time in 2000, and continued to constitute a challenge in energy technologies in the past decade. RESD is mainly interested in case studies of sustainable development and its relation to transition economies in the Middle East, Africa, Asia and Oceania.

RESD has an outstanding editorial board of eminent scientists, researchers and engineers who contribute and enrich the journal with their vast experience in different fields of interest to the journal. The journal is open-access with a liberal Creative Commons Attribution-Non Commercial-4.0 International License. Which preserves the copyrights of published materials to the authors and protects it from unauthorized commercial use or derivation. The journal is financially supported by Arab Academy for Science, Technology and Maritime Transporting in order to maintain quality open-access source of research papers on renewable energy and sustainable development.

Editorial Committee

Administrative Board

Contents

Articles

Journal of Renewable Energy and Sustainable Development (RESD) Volume 8, Issue 2, December 2022 - ISSN 2356-8569
http://dx.doi.org/10.21622/RESD.2022.08.2.035

Received on, 07 June 2022 Accepted on, 13 July 2022 Published on, 10 August 2022

Geospatial Assessment Of Small Hydropower Potentials In Ogun Watershed For Rural Electrification

Olaide Sheerifdeen Akande[1], Yekeen Adeeyo Sanusi[1], Lekan Mohammed Sanni[1] & Idris-Nda Abdullahi[2]

[1]Department of Urban and Regional Planning, Federal University of Technology, Minna
[2]Department of Geology, Federal University of Technology, Minna

olaide.akande@futminna.edu.ng, yasanusi@futminna.edu.ng, sanni.lekan@futminna.edu.ng, idrisnda@futminna.edu.ng

ABSTRACT

Energy access is one of the challenges confronting Nigeria and many Sub-Saharan African countries. The energy poverty experienced in the country is even more pervasive in the rural communities where only about 36% of the population had access to electricity. With the current improvement in technological advancement in GIS and remote sensing, identifying small hydropower sites have become relatively easier, faster, and cost effective. Small hydropower is a clean renewable and reliable energy alternative that meets the economic and environmental energy policy objectives. This study therefore seeks to explore the viability of the SHP potentials for rural electrification.The quantitative research approach was employed.

The study analysed the small hydropower potentials in Ogun watershed using geospatial techniques (Hydrology, Neighbourhood analysis, Watershed analysis) and descriptive statistics to describe the population and energy dynamics of the study area. The study identified a total of 137 potential hydropower sites with a minimum energy potential of 502 kw and a maximum of 5.80 mw. Ogun watershed that has 202200 kW of potential energy is expected to support the electricity need of 59,471 rural households across ten local government areas in Ogun watershed.

The study concludes that with the abundant water resources available in the country, small hydropower plants are a viable option for reducing the energy deficit of the country and can also help in the attainment of sustainable development goal 7 (universal energy access for all). The study further posited that the development of small hydropower in Ogun Watershed reduces the level of energy poverty experienced in the rural communities and stimulates the growth and development of the communities across social, environmental, and economic dimension.This study was able to estimate the viability of the energy potential identified along Ogun Watershed for rural electrification of communities within 2 km radius of the potential site.

Index-words: *Electricity, GIS, Rural Electrification, Small hydropower potential.*

I. BACKGROUND

Access to electricity supply is fundamental to the achievement of any meaning development in a nation. However, over two billion people across the world lack access to electricity (International Energy Agency (IEA), 2018). More than 620 million people in Sub-Saharan Africa (SSA) are believed to be without power (IEA, 2014) and about 60% of Nigerians do not have access to electricity despite the abundant energy resources available in the country (IEA, 2019). Going by the current electricity deficit and population growth projections, the number of people worldwide without access to electricity may surpasses 2.5 billion people by 2030 if current electricity supply and distribution is not improved (IEA, 2017).

In Nigeria, there is the rural urban dichotomy on electricity access. According to the International Energy Agency (2016), electricity access in Nigeria is at 55 percent in urban areas and 36 percent in rural areas, while about 134 million people (76 percent) rely on traditional biomass for energy. Majority of the population without access to electricity are located in the country's rural areas, far away from existing and usually poor grid network. Extending electricity to these communities (rural communities) come with huge investments, structural, and technological changes in energy system (Barnes, 2005; Alexandros et al., 2018). Therefore, if these challenges must be overcome, a more flexible and sustainable electrification scheme must be developed in a cost-effective manner (Mentis, 2016).

Hydropower is among the most efficient technologies for production of renewable electrical energy, with

http://dx.doi.org/10.21622/RESD.2022.08.2.035

a typical efficiency of 90% (Killingtveit, 2019). In 2015, 16.6% of electricity produced worldwide comes from hydropower. Currently, hydropower accounts for 17% of the electricity generation in Africa on average (IEA, 2020). Installed electricity capacity of hydropower as of 2017 was 30.4 GW in sub-Sahara Africa, yet 92% of the potential capacity of 300 GW remains untapped (Zhou et al., 2015). Similarly, only about 20% of Nigeria's electricity generation comes from hydropower, mostly large hydropower plants (Kainji, Shiroro, and Jebba hydropower dam). The development of large hydropower plant takes time, requires huge investment, and comes with social and environmental implications or dislocations (Nautiyal, 2012). The current economic challenges faced in the world in general and in Nigeria in particular make investment in large hydropower generation plants become difficult.

Opportunities to improve hydropower electricity generation in most remote areas abound in Africa, especially when developed in small and decentralized scale (Stockholm Environment Institute, 2016). In the presence of current hydrological conditions, small hydropower offers huge opportunities for electricity generation with less cost, time and little or no social and environmental implications (Yadoo and Cruickshank, 2012). Among all non-conventional renewable energy sources, small hydropower (SHP) has the highest density and ranks first in the generation of electricity from renewable sources around the world (Dudhani, et al., 2006). SHP can operate in both isolated and interconnected (connect to nation grid) mode (Yadoo and Cruickshank, 2012). In lieu of the numerous advantages of SHP, Szabo et al. (2011) argued that small-scale hydro is a very suitable option for rural electrification in Africa.

The identification and development of SHP sites have become much faster, cheaper, and cost effective with the advancement in technology, particularly Geographic Information System (GIS). The use of GIS and remote sensing data have been exemplified in local and international studies (Feizizadeh and Haslauer, 2012; Alaxandros et al., 2019, Fasipe and Izinyon, 2021). However, these studies reflect only on the availability of energy potential along river basins and watershed without matching it with energy demand of communities within a reasonable distance. Providing information on the viability of the energy potentials within the source area can stimulate private and government investment in small hydropower plant development. This study is therefore an attempt to showcase a pathway towards effective geospatial assessment of small hydropower potentials and viability for electricity generation in Ogun watershed. The objectives of the study are to:

1. Assess the characteristics of perennial rivers within the watershed;
2. Examine small hydropower potential sites;
3. Examine the energy situation of communities within 2 km radius of the SHP sites; and
4. Determine the viability of the potential SHP sites.

II. LITERATURE REVIEW

A. *Concept of Small Hydropower*

Water has been exploited as a source of energy by industry and a small number of utility providers for generations. The creation of hydroelectric electricity on a small scale to serve a local community or industrial operation is known as small hydro (Bhatia, 2014). The definition of a small hydro project varies, although it is widely considered that a producing capacity of up to 10 megawatts (MW) is the upper limit. This might be increased to 30 MW in the US and 50 MW in Canada (Khare et al., 2019). A hydropower plant can be further classified into a mini hydro, which is defined as a plant with an installed capacity of less than 1000 kW, and a micro hydro, which is defined as a plant with an installed capacity of less than 100 kW. A micro hydro is a type of hydroelectric electricity that is designed for a smaller town, single families, or small businesses.

B. *Application of GIS and Remote Sensing to SHP Survey*

Sammartano et al. (2019) identified potential locations of hydropower plants using GIS-based procedure in the Taw at Umberleigh catchment, Southwest England. River flows were used to estimate the river flows for flow duration curve assessment. In order to find suitable hydropower locations in the Mahanadi River basin, Goyal et al. (2015) employed a multi-criteria approach that combined an advanced methodology for geospatial raster/grid data preparation with the SWAT model (India). Kusre et al. (2010) used GIS technologies with the Soil and Water Assessment Tool (SWAT) hydrological model to assess the hydropower potential of a large basin in India, identifying a large number of possible hydropower sites. Pandey et al. (2015) also employed SWAT inside a GIS framework to analyze water availability for hydropower in India's Mat River basin. The SWAT model has been widely utilized to simulate hydrological processes in a variety of research, resulting in accurate river flow estimates in ungauged basins (Stehr et al., 2008; Memarian et al., 2014; Omani et al., 2017).

C. *Energy Consumption Pattern in Ogun State and Other Regions of the World*

According to IBEDC (2017), the average electricity consumption per annum in Ogun State is 7.5x107

http://dx.doi.org/10.21622/RESD.2022.08.2.035

kWh. This translates to an average of 27 kWh (Table 1) per capita per annum. The annual per capita energy consumption is only about 19% of the national average of 145 kWh. This is an indication of the level of energy poverty experienced in Ogun State, particularly in the rural areas beyond the reach of the poor electricity distribution network. The average electricity consumption in Sub-Saharan Africa is 487 kWh, 705 kWh in South Asia, 6022 kWh in European Union countries and 13254 in North America (IEA, 2014). According to IEA (2014), the world electricity consumption is estimated as 3128 kWh. Based on the foregoing analysis, it can be observed that only 5.7% of Sub-Saharan Africa's average electricity consumption is available to residents in Ogun state, 1.7% of European countries, 0.2% of North America, and 0.9% of the world electricity consumption average. Indeed, this poor performance in energy access has great implication on the social and economic development of the people, particularly the rural populace. There is need for improved electricity generation and distribution in Ogun State in particular and Nigeria at large if the sustainable development goal 7 (SDG 7) must be achieved before 2030.

TABLE I: AVERAGE REGIONAL ELECTRICITY CONSUMPTION PATTERN IN THE WORLD

Regions	Avg. Electricity Consumed per capita (kWh)	Source	Relative
Ogun State	27.6	Ibadan Electricity Distribution Company (IBEDC, 2017)	0
Nigeria	120-145	Worlddata.info; IEA, 2014	19.0
Sub-Sahara Africa (excluding South Africa)	180	African Development Bank Group (ADBG, 2022)	5.7
South Asia	705	IEA, 2014	3.9
East Asia and the Pacific	3665	IEA, 2014	0.8
North America	13254	IEA, 2014	0.2
Europe	1581	Eurostat, 2019	1.7
European Union	6022	IEA, 2014	0.5
World	3128	IEA, 2014	0.9

III. STUDY AREA AND METHODOLOGY

A. Study Area

Ogun State is one of the thirty-six states of Nigeria and it is located in the southwest region of the country (Figure 1). Ogun State is bordered by the former capital of Nigeria, Lagos state to the south, Oyo and Osun States to the North, Ondo State, and Republic of Benin to the west. Abeokuta is the administrative Capital of Ogun State and is the most populous city in the state. It has an estimated land area of 16,762 km2 and a projected population of 6.15 million people as at the end of 2021. Ogun State has high concentration of industries notable among which are Dangote cement and Coleman Cables among others. The high population of people and industries imply high demand for energy for domestic and industrial use. The major rivers in Ogun state include Rivers Ogun, Osun, Oyan and Oni. Ogun State has a tropical climate in general. The average monthly temperature varies from 23°C in July to 32°C in February, with the wet season lasting from March to November and the dry season lasting from December to February (Azodo, 2014). Because of the high temperature in the area, electric fans and air conditioners are required for space cooling.

http://dx.doi.org/10.21622/RESD.2022.08.2.035

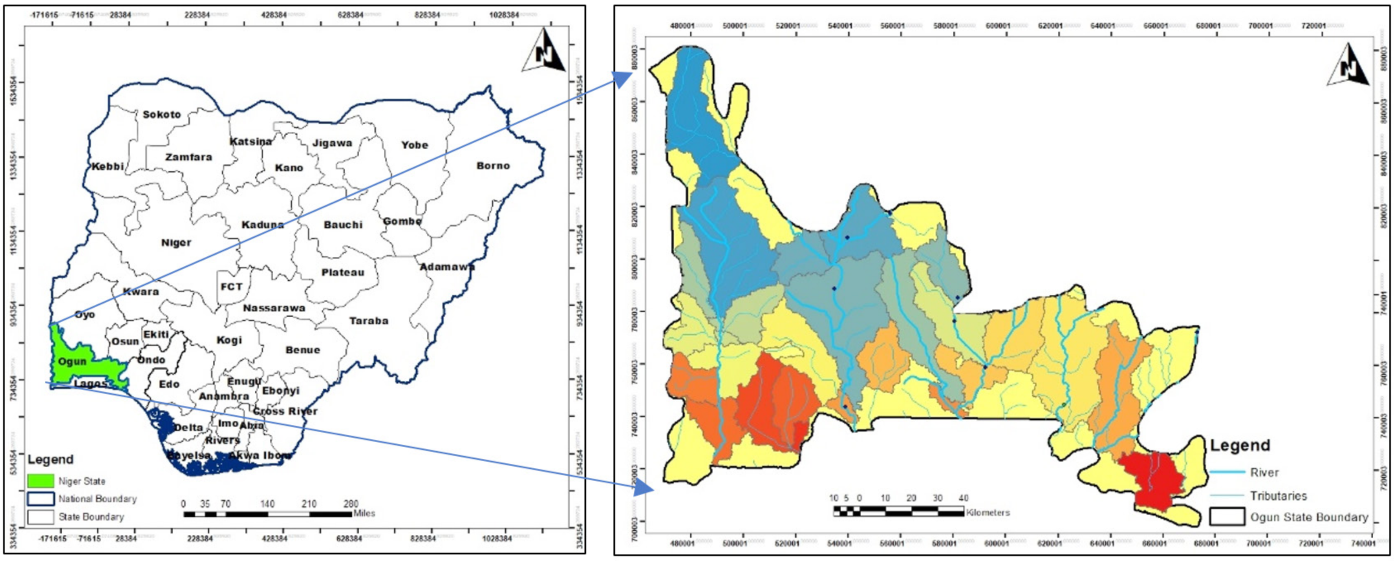

Fig. 1. Ogun State Watershed in the Context of Nigeria

B. Methodology

The concept of hydropower is predicated on the ability of water to be dropped from a high level to a low level, the pressure that emanates from this fall can be converted to mechanical energy which can be used to drive electric generator (Fraenkel et al., 1991). In this study, hydropower potential sites were identified using GIS and remote sensing approach. Shuttle Radar Topographic Mission (SRTM) was downloaded form United States Geological Survey (USGS) from which the Digital Elevation Model (DEM) of high spatial resolution of 0.00083 degrees was derived. The overall value of theoretical hydropower potential for that place is computed by adding up each individual hydropower value (based on equiareal raster cells). The DEM derived was masked with the administrative boundary of the study area. The DEM was load into ArcGIS 10.8 environment for spatial analysis. The spatial analyst tools used include hydrology, map algebra, neighbourhood, and conditional function tools. The DEM was subjected to fill, flow direction, and flow accumulation function under the hydrology tool to derive the amount of runoff per raster cell (m). Stream networks in elevation models are defined using the flow accumulation function. The accumulated flow is calculated using the weight of each cell flowing into each raster cell. Higher flow accumulation values represent sinks in a given location, and lower accumulation values represent peaks. In this example, the accumulation raster is weighted by the amount of potentially available water in the area under consideration, which is represented by the direct runoff data's integer dataset. The sum of water accumulated in each raster cell, which corresponds to the mass of water (m), is the output of the flow accumulation function (density of water x runoff).

Secondly, on the digital elevation data, a focal statistics function is used. This is a function that computes the necessary statistics (i.e., minimum, maximum, total of all values) for the cells that surround each particular cell. The minimal function in modern analysis is applied to a rectangle containing 3*3 cells around each cell which are used to find the minimum cells around each raster cell (lowest neighbouring cells). Consequently, the derive minimum neighbours were subtracted from the DEM to determine the drop in elevation of each cell to its minimum neighbours (gradient of fall). The output is called the "head" which is the height value and one of the variables required for the calculation of potential energy. Using the energy equation advanced by Carroll et al. (2004) which is mathematically expressed in equation (1), the energy potential of the identified site was derived.

(1) E= m * g * h

*Note: The output dimension is in Joules which then has to be transformed to kWh and MW h by using the calculation factor (1/3.6 * 1012)*

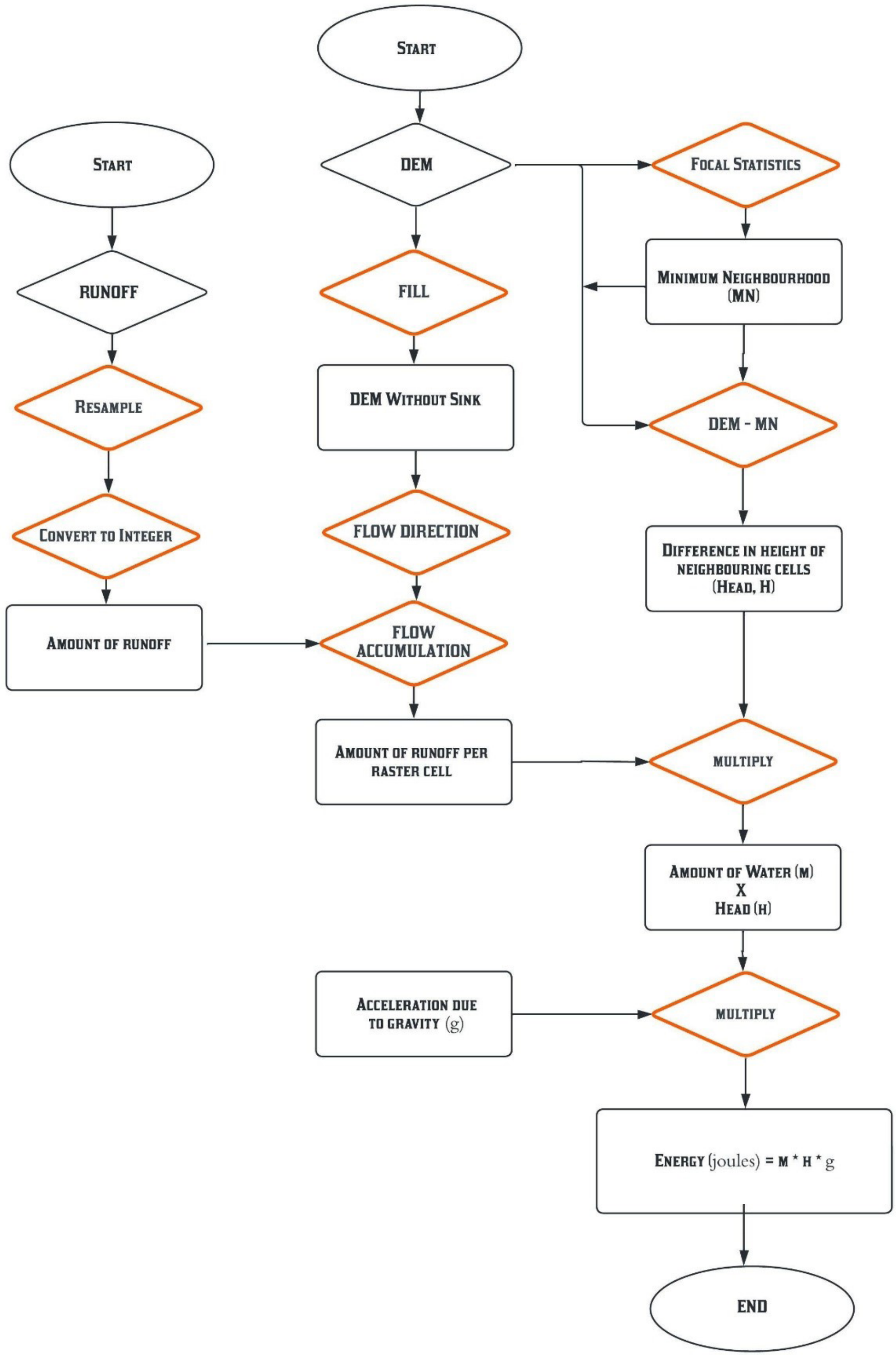

Fig. 2. Flow Chart of the Research Methodology
Source: Adapted from Feizizadeh and Haslauer (2012)

1. *Estimating Electricity Threshold Required to Meet SDG 7*

Energy reliability, affordability, and sustainability are the key goals of Sustainable Development Goal 7. However, it does not set the minimum per capita energy threshold to be achieved to ensure energy access for both residential and non-residential sector. Hence, there is no universally acceptable electricity consumption threshold; electricity access threshold varies across countries and continents of the world. For example, Moss et al. (2020) proposed a minimum energy benchmark of 1000kWh per capita per annum inclusive of residential (300 kWh) and non-residential (700 kWh) electricity consumption for the achievement of SDG 7. IEA (2015) also proposed a minimum threshold of 250 and 500 kWh/year for rural and urban households (assumed to be five persons), respectively. Similarly, Brecha (2019) also argued that a minimum electricity threshold of at least 400k Wh is close to meeting the outcomes of SDG 7. Based on the economic dynamics and rural nature of most communities within five-kilometre radius of the identified SHP potential sites in Ogun State, the IEA minimum threshold value of 250 kWh per household (five persons) will be adopted as the minimum energy threshold for energy analysis in Ogun Watershed.

IV. RESULTS AND DISCUSSION

A. Characteristics of the River Channel

The study identified and ground trothed six permanent and perennial rivers in Ogun State. These are Rivers Ogun, Oshun, Oyan, Oni, and two rivers with unknown name and hence were named unknown I, and unknown II. The length of the six Rivers ranges from 12.4km – 79km. The minimum elevation level along the six Rivers ranges from 3.4 m – 21.8 m, while a maximum elevation range of 74.0 m – 214.4 m (Table 2). The slope characteristics of the rivers in degrees ranges from 0.000804 - 0.001778. Based on the slope characteristics along the stream, a total of 137 potential small hydropower potential sites were identified. Fifty-five (55) of the potential sites were identified along River Ogun, 32 and 19 on River Oshun, and Oyan respectively. The “unknown” Rivers had 24 potential sites cumulatively, and 7 potential sites on River Oni. The results revealed that the development of small hydropower plant will be more viable on Rivers Ogun and Oshun owing to the large number of potential sites available along the water channel.

TABLE II: CHARACTERISTICS OF STREAM NETWORK IN OGUN WATERSHED

River	Stream length in km	Max Elev (m)	Min Elev (m)	No Hydropower Site	Average Bed Slope
OGUN	79	214.4	15.1	55	0.000804
OYAN	24.4	91	33.7	19	0.001554
Unknown I	17.6	76.1	16.8	8	0.001778
OSHUN	58.2	84.2	3.4	32	0.001256
Unknown II	36	74	14.8	16	0.001534
ONI	12.4	107.3	21.8	7	0.001464
Total				137	

Note: Elev= Elevation

B. Potential Small Hydropower Sites in Ogun Watershed

The potential small hydropower energy sites identified in Ogun watershed along the six primary streams identified in Ogun watershed is presented in Table III. The study established that about 224.7 MW of electricity can be generated from the watershed. The minimum energy potential along the river channels is 500 kW along river Ogun, and a maximum of 5.80 MW on the same stream. Ogun River had a potential energy of 75.4 MW, Oshun 67.5 MW, and 20.4 MW from River Oyan. These three Rivers accounted for about 81% of the potential energy estimated in the watershed. Potential energy identified along unknown River I and II are 5 MW and 26.3 MW respectively, while potential energy of 7.6 MW was estimated along Oni River. Table III further shows the average distance between the identified potential sites of the small hydropower plants. The average spacing between the potential sites ranges from a minimum of 1.61 km along River Oyan to a maximum of 2.2 km along Unknown River I. The spatial distribution of the potential small hydropower sites is depicted in Figure 3.

http://dx.doi.org/10.21622/RESD.2022.08.2.035

TABLE III: DISTRIBUTION OF ENERGY POTENTIALS IN OGUN WATERSHED

River	MIN (MW)	MAX (MW)	PWR_(MW)	Ave. Spacing between plants
OGUN	0.502	5.798	75.4	1.74
OYAN	0.573	7.24	20.4	1.61
UNK River I	0.512	0.926	5.01	2.2
OSHUN	0.529	5.483	67.5	1.88
UNK River II	0.533	2.912	26.3	2.25
ONI	0.516	1.519	7.6	1.77
Total			**202.2**	

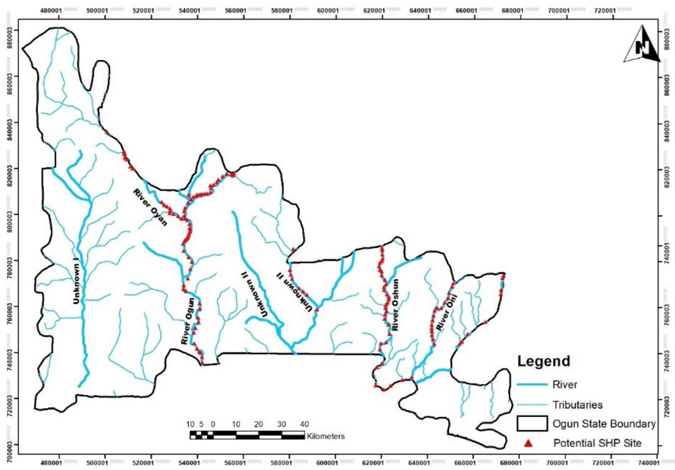

Fig.3. Spatial Distribution of Small Hydropower Potential Sites

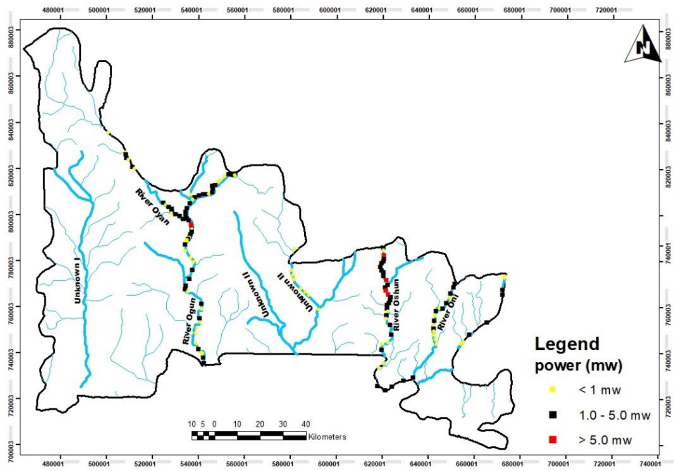

Fig 4. Classess of Small Hydropower Potential Sites in Ogun Watershed

The potential small hydropower sites identified were classified into three; less than 1 MW (1000 Kilowatts), 1-5 mw, and above 5 MW. Table IV shows the three classes of hydropower sites. A total of 59 sites had electricity potential of less than 1 MW (1000 kWh) with a cumulative energy potential of 39.5 MW, 73 SHP sites had between 1-5 MW electricity potential and cumulative energy potential of 136 MW, while only five SHP sites had electricity potential of more than 5 MW but less than 10 MW and a cumulative energy potential of 26.7 MW. Four of the five potential sites were located along river Oshun and one on river Ogun. The spatial distribution pattern of the potential hydropower site based on the three categories identified is depicted in Figure 4.

TABLE IV: NUMBER OF SMALL HYDROPOWER SITES BY CATEGORY OF ENERGY POTENTIALS

River	Frequency	Percent	Cumulative Energy Potential (MW)
Below 1 mw	59	43	39.5
1.0 – 5.0 mw	73	53	136
Above 5 mw <10mw	5	4	26.7
Total	**137**	**100**	**202.2**

C. Energy Access Situation of Communities along Rivers in Ogun Watershed

A total of 76 communities were identified within 2 km radius of the six rivers (Table V).. Therefore, the connection to grid and average daily electricity access of the communities were assessed. The result revealed that 73 of the total communities identified were rural, mostly hamlets and small villages, while three communities were urban. It is instructive to report that the 73 rural communities along the river course were not connected to the national grid and hence do not have access to public electricity. Only the urban communities along the river course were connected to the national grid. The study also established that only an average of 3-6 hours of electricity is enjoyed daily in the urban communities intermittently during the day. This shows that all the communities within two-kilometre radius of the potential SHP sites are energy poor. Therefore, demand for electricity within reasonable distance of the SHP sites is expected from the communities.

http://dx.doi.org/10.21622/RESD.2022.08.2.035

TABLE V: ENERGY SITUATION OF COMMUNITIES ALONG THE RIVERS IN OGUN WATERSHED

River	Communities	E.A Status	Daily Duration of Electricity
Rural	73 (96%)	Not Connected	0
Urban	3 (17%)	Connected	3-6
Total	**76 (100%)**		

D. Estimated Rural Household Population that can be Connected in Ogun Watershed

Small hydropower potential sites are distributed across ten of the twenty Local Government Areas (LGAs) in Ogun State. The study provides an insight into the possible number of households (average of five members) that can be provided with a minimum energy threshold of 250 kWh on a daily basis. This is equivalent to an average daily electricity access of 0.68 kWh per capita and 3.4 kWh per household per day. The number of households that can be served with the electricity potentials estimated within the ten LGAs is provided in Table VI. The energy potentials estimated in Ogun watershed can support 59,471 households at 100% performance of the potential sites. In Ijebu east LGA, 20,059 households can be provided with minimum energy of 250 kWh and this population is equivalent to 59.8% of the projected household population in the LGA. The energy potentials in Ijebu North, Odeda, and Abeokuta North can support a minimum household population of 10,382, 9,265, and 7,206, respectively. The energy potentials available in Odogbolu LGA can support a minimum of 147 households which is equivalent to only about 0.4% of the projected household population. The energy potentials estimated in the LGAs can support a population of 297355 persons with minimum energy services like lighting, fan, phones, and television. This will no doubt provide opportunity for many households in the remote communities within the services radius of the potential sites to have access to electricity and hence reduce energy poverty within the LGAs, and Ogun watershed at large.

TABLE VI: ESTIMATED RURAL HOUSEHOLD POPULATION THAT CAN BE ELECTRIFIED

LGAs	Prj. HH POP	Energy Potential (kWh)	Est HH to be served	% HH POP
Abeokuta South	61047	9900	2,912	4.8
Abeokuta North	76862	24500	7,206	9.4
Odeda	33633	31500	9,265	27.5
Obafemi Owode	72187	11900	3,500	4.8
Ifo	165572	10500	3,088	1.9
Remo north	18349	1900	559	3.0
Ijebu North	86144	35300	10,382	12.1
Ijebu East	33571	68200	20,059	59.8
Imoko East	25473	8000	2,353	9.2
Odegbolu	38588	500	147	0.4
Total	**611425**	**202200.0**	**59, 471**	**9.7**

Prj = Projected; HH= Household; POP= Population

http://dx.doi.org/10.21622/RESD.2022.08.2.035

V. CONCLUSION AND RECOMMENDATIONS

The results have shown that GIS and remote sensing data can provide the requisite technology needed to identify potential sites in a cheaper and simpler manner and within a reasonable period of time. This is a much better approach to the traditional water resources assessment approach using discharged data at the outlet of watershed. The available small hydropower potentials estimated in Ogun Watershed is expected to stimulate efforts towards identifying small hydropower potentials in the country with a view to harnessing the same for rural electrification, especially with the increasing demand for clean and sustainable energy. Based on the current energy situation of the communities identified within 2 km radius of the site, the potential energy from the SHP sites are economically viable for development by government and private investors. The development of the small hydropower potentials is estimated to provide a minimum of 250 kWh for up to 59,471 households in Ogun Watershed. This implies that SHP within this area can serve as a tool for energy poverty and carbon footprint reduction in the communities identified. Harnessing the small hydropower potential across the country provides a huge prospect for the attainment of SDGs 7 and 13 and facilitates the achievement in education, health, and production, thereby leading to increase the wellbeing of the population and higher gross domestic product for the country. This study therefore recommends the decentralization of electricity generation in the country in order to allow for adequate investment in small hydropower potentials across the 36 states of Nigeria. The government must also take advantage of the technological advancement, particularly in GIS and remote sensing for small hydropower assessment in order to facilitate the identification and estimation of small hydropower potentials in a cost effective and sustainable manner.

REFERENCE

[1] A. P. Azodo, "Electric power supply, main source and backing: A survey of residential utilization features," International Journal of Research Studies in Management, vol. 3, no. 2, 2014, doi: 10.5861/ijrsm.2014.880.

[2] D.F. Barnes., Meeting the Challenge of Rural Electrification in Developing Nations: The Experience of Successful Programs. Washington, DC.: Energy Sector Management Assistance Program (ESMAP), 2005.

[3] R. Brecha, "Electricity Access Threshold for Meeting Non-Energy SDG Targets," European Journal of Sustainable Development, vol. 8, no. 4, 2019, doi: 10.14207/ejsd.2019.v8n4p90.

[4] S. M. Carroll, V. Duvvuri, M. Trodden, and M. S. Turner, "Is cosmic speed-up due to new gravitational physics?," Physical Review D - Particles, Fields, Gravitation and Cosmology, vol. 70, no. 4, 2004, doi: 10.1103/PhysRevD.70.043528.

[5] S. Dudhani, A. K. Sinha, and S. S. Inamdar, "Assessment of small hydropower potential using remote sensing data for sustainable development in India," Energy Policy, vol. 34, no. 17, 2006, doi: 10.1016/j.enpol.2005.06.011.

[6] O. A. Fasipe and O. C. Izinyon, "Feasibility assessment of SHP potential using GIS-enhanced RS approach in poorly gauged river basin in Nigeria," Renewable Energy Focus, vol. 36, 2021, doi: 10.1016/j.ref.2020.12.005.

[7] B. Feizizadeh and E. Haslauer, "GIS-based procedures of hydropower potential for Tabriz basin, Iran," 2012.

[8] P. Fraenkel, O. Parish, V. Bolkalders, A. Harvey, A. Brown, and R. Edwards, "1. Micro-hydro Power," in Micro-hydro Power, 1991. doi: 10.3362/9781780442815.001.

[9] Y. Goyal, M. S. Arya, and S. Nagpal, "Energy efficient hybrid policy in green cloud computing," 2016. doi: 10.1109/ICGCIoT.2015.7380621.

[10] Ibadan Electricity Distribution Company (IBEDC), "Ibadan Electricity Distribution Company Annual report," 2017.

[11] Key World Energy Statistics 2014. Paris: International Energy Agency (IEA) , 2014. Accessed: Feb. 03, 2022. [Online]. Available: https://www.iea.org/reports/key-world-energy-statistics-2014

[12] World Energy Outlook 2015. Paris: International Energy Agency (IEA) , 2015. Accessed: Feb. 03, 2022. [Online]. Available: https://www.iea.org/reports/world-energy-outlook-2015

[13] World Energy Outlook 2016. Paris: International Energy Agency (IEA) , 2016. Accessed: Feb. 03, 2022. [Online]. Available: https://www.iea.org/reports/world-energy-outlook-2016

[14] Energy Access Outlook 2017. Paris: International Energy Agency (IEA) , 2017. doi: 10.1787/9789264285569-en.

[15] World Energy Investment 2018: Executicve Summary. Paris: International Energy Agency (IEA) , 2018. Accessed: Feb. 03, 2022. [Online]. Available: https://www.iea.org/reports/world-energy-investment-2018

[16] Africa Energy Outlook 2019 - Overview Nigeria. Paris: International Energy Agency (IEA), 2019.

http://dx.doi.org/10.21622/RESD.2022.08.2.035

Accessed: Feb. 03, 2022. [Online]. Available: https://www.iea.org/articles/nigeria-energy-outlook

[17] Climate Impacts on African Hydropower. OECD, 2020. doi: 10.1787/7f8fc476-en.

[18] V. Khare, S. Nema, and P. Baredar, "Reliability analysis of hybrid renewable energy system by fault tree analysis," Energy and Environment, vol. 30, no. 3, 2019, doi: 10.1177/0958305X18802765.

[19] Å. Killingtveit, "Hydropower," in Managing Global Warming: An Interface of Technology and Human Issues, 2018. doi: 10.1016/B978-0-12-814104-5.00008-9.

[20] B. C. Kusre, D. C. Baruah, P. K. Bordoloi, and S. C. Patra, "Assessment of hydropower potential using GIS and hydrological modeling technique in Kopili River basin in Assam (India)," Applied Energy, vol. 87, no. 1, 2010, doi: 10.1016/j.apenergy.2009.07.019.

[21] H. Memarian, S. K. Balasundram, K. C. Abbaspour, J. B. Talib, C. T. Boon Sung, and A. M. Sood, "SWAT-based hydrological modelling of tropical land-use scenarios," Hydrological Sciences Journal, vol. 59, no. 10, 2014, doi: 10.1080/02626667.2014.892598.

[22] D. Mentis et al., "The benefits of geospatial planning in energy access - A case study on Ethiopia," Applied Geography, vol. 72, 2016, doi: 10.1016/j.apgeog.2016.04.009.

[23] T. Moss et al., "The Modern Energy Minimum: The case for a new global electricity consumption threshold," Energy for Growth Hub, 2020.

[24] H. Nautiyal and Varun, "Progress in renewable energy under clean development mechanism in India," Renewable and Sustainable Energy Reviews, vol. 16, no. 5. 2012. doi: 10.1016/j.rser.2012.02.008.

[25] N. Omani, R. Srinivasan, P. K. Smith, and R. Karthikeyan, "Glacier mass balance simulation using SWAT distributed snow algorithm," Hydrological Sciences Journal, vol. 62, no. 4, 2017, doi: 10.1080/02626667.2016.1162907.

[26] A. Pandey, D. Lalrempuia, and S. K. Jain, "Assessment of hydropower potential using spatial technology and SWAT modelling in the Mat River, southern Mizoram, India," Hydrological Sciences Journal, vol. 60, no. 10, 2015, doi: 10.1080/02626667.2014.943669.

[27] V. Sammartano, L. Liuzzo, and G. Freni, "Identification of potential locations for run-of-river hydropower plants using a GIS-based procedure," Energies (Basel), vol. 12, no. 18, 2019, doi: 10.3390/en12183446.

[28] A. Stehr, P. Debels, F. Romero, and H. Alcayaga, "Hydrological modelling with SWAT under conditions of limited data availability: Evaluation of results from a Chilean case study," Hydrological Sciences Journal, vol. 53, no. 3, 2008, doi: 10.1623/hysj.53.3.588.

[29] W. Russel, "Renewable energy mini-grids: An alternative approach to energy access in southern Africa," JSTOR, 2016.

[30] S. Szabó, K. Bódis, T. Huld, and M. Moner-Girona, "Energy solutions in rural Africa: Mapping electrification costs of distributed solar and diesel generation versus grid extension," Environmental Research Letters, vol. 6, no. 3, 2011, doi: 10.1088/1748-9326/6/3/034002.

[31] "United State Geology Survey (USGS)." www.usgs.com

[32] A. Yadoo and H. Cruickshank, "The role for low carbon electrification technologies in poverty reduction and climate change strategies: A focus on renewable energy mini-grids with case studies in Nepal, Peru and Kenya," Energy Policy, vol. 42, 2012, doi: 10.1016/j.enpol.2011.12.029.

[33] Y. Zhou et al., "A comprehensive view of global potential for hydro-generated electricity," Energy and Environmental Science, vol. 8, no. 9. 2015. doi: 10.1039/c5ee00888c.

Journal of Renewable Energy and Sustainable Development (RESD)
Volume 8, Issue 2, December 2022 - ISSN 2356-8569
http://dx.doi.org/10.21622/RESD.2022.08.2.045

Received on, 07 September 2022 Accepted on, 07 October 2022 Published on, 26 October 2022

Three-dimensional CFD Analysis of PEMFC with Different Membrane Thicknesses

Mahmut Kaplan

Department of Machine and Metal Technology, Naci Topcuoglu Vocational High School, Gaziantep University, Gaziantep, Turkey

mahmutkaplan@gantep.edu.tr

ABSTRACT

PEM fuel cell (PEMFC) is a potential candidate for future source of power used in different applications such as transportations, stationary and portable power. PEMFC consists of different parts including membrane, bipolar plate, flow channel, gas diffusion and catalyst layers. Membrane is one of the most important components of a PEMFC and its physical and geometrical features significantly affect PEMFC efficiency. In this paper, a three-dimensional, single-phase computational model has been improved to scrutinize membrane thickness effect on the PEM fuel cell performance using the ANSYS PEM Fuel Cell Module.

Membrane thicknesses are in the range of 0.0127 to 0.189 mm. The results reveal that a decrease in membrane thickness augments the current density at 0.4 and 0.6 V. The peak current density of 3.12 A/cm^2 is achieved with 0.027 mm membrane thickness compared with the model current density of 1.26 A/cm^2 obtained by the model with 0.128 mm membrane thickness at 0.4 V. Oxygen consumption. Water production is also enhanced with reducing membrane thickness to 0.4 and 0.6 V. However, the changed thickness of the membrane has a negligible impact on impact pressure drop in the flow channel. It is found that optimization of membrane thickness is necessary for attaining high efficiency.

Index-words: *PEMFC, Membrane thickness, CFD, Cell performance, Pressure drop, Optimization.*

I. INTRODUCTION

The use of fossil fuels for power has resulted in many adverse impacts including climate change and air pollution. The interest in proton exchange membrane fuel cell (PEMFC) has grown noticeably because of the requirement for clean energy. The potential applications of the PEMFC are transportation (cars, trains, boats, planes and drones), stationary and portable power sectors (Wu, 2016).

Basic components of PEMFC are gas diffusion layer (GDL), catalyst layer (CL), membrane and flow channel (Xing et al., 2019). In a PEMFC, hydrogen as a fuel is converted electrochemically into electricity. During the PEMFC operation, molecular hydrogen (H_2) from anode gas flow channel is oxidized on the anode CL ($H_2 \rightarrow 2H^+ + 2e^-$) and hydrogen ions pass through the membrane. Meanwhile the electrons flow through GDL to the anode current collector and arrive by means of the cathode current collector. Oxygen is reduced by reaction between the electrons, the hydrogen ions, and oxygen supplied from cathode gas flow channel ($O_2 + 4H^+ + 4e^- \rightarrow 2H_2O$).

In order to operate PEMFC efficiently, membrane must satisfy the needs such as high proton conductivity, an adequate barrier to the reactants chemically and mechanically stable (Barbir, 2013). Improving computational model of PEMFC helps to investigate the efficiency of membrane for different operating and geometrical parameters. Compared to experimental studies, computational models provide detailed information and save time and cost. Recently, several studies have been conducted to evaluate impacts of membrane geometry and materials property on PEMFC efficiency (Iranzo et al. 2014; Nishimura et al., 2021; Luo et al., 2021; Kienitz, 2021).

Iranzo et al. (2014) developed a three-dimensional numerical model to scrutinize the impact of the membrane thermal conductivity on cell performance using ANSYS Fluent. It was found that an increase in the membrane thermal conductivity leads to decreasing membrane temperature and augmenting protonic conductivity and cell electric power.

Nishimura et al. (2021) studied impacts of various thicknesses of membrane on the power generation performance of PEMFC using the commercial software Comsol Multiphysics. Their results showed the thinner membrane promoted the current density because of enhancing water flux and conductivity of membrane. Luo et al. (2021) conducted experimental work to determine the impacts of membranes within thicknesses ranging from 5 µm to 70 µm on the structure and characteristics of membrane. Their findings revealed that below a certain thickness (<10 µm), membranes exhibited considerable change in their structure and features associated with increasing anisotropy and swelling.

Mohanty et al. (2021) analyzed the influences of membranes having different thicknesses (2, 3.5 and 5 mil) on PEMFC performance using COMSOL Multiphysics software. It was concluded that membranes with 2 mm thickness developed the cell performance by 17%, thanks to decreasing internal resistance compared to other thicknesses. Kienitz (2021) improved a new numerical model to optimize membrane thickness for automotive hydrogen PEMFC systems. The results showed that the model was capable of estimating optimal membrane thickness but this thickness is dependent on operating conditions.

The objective of this investigation is to study the interrelationship between membrane thickness and the PEMFC efficiency using a single-phase computational fluid dynamics (CFD) model improved in the previous work (Kaplan, 2021). The outcomes of the work can help geometry optimization in PEMFC design. Besides, the suggested model can be used to improve reactants utilization in PEMFC.

II. COMPUTATIONAL METHOD

SOLIDWORKS is used to produce the geometry of PEMFC. Then the geometry is imported the Fluid Flow Analysis System in ANSYS Workbench Platform (ANSYS, 2018). The structured mesh is generated in Meshing. As shown in Figure 1, the mesh must consist of nine elements including anode and cathode GDL, CL, flow channel and membrane in order to identify the properties of these elements in the ANSYS FLUENT Fuel Cell Module.

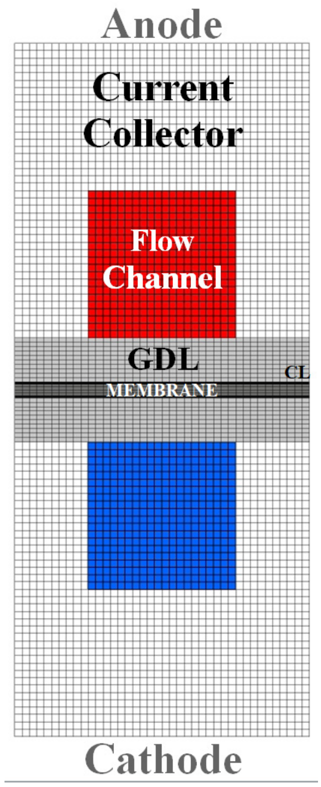

Fig. 1. Meshing of PEMFC model

Model geometrical parameters based on Wang et al.'s experimental study are presented in Table I.

TABLE I. GEOMETRICAL PARAMETERS FOR THE MODEL (Wang et al., 2003)

Parameter	Value
Cell width	2 mm
Cell length	70 mm
Channel width and	1 mm
GDL thickness	0.3 mm
CL thickness	0.0129 mm
Membrane thickness	0.108 mm

In the present study, the mass, momentum, species and energy equations are employed in the PEMFC model. Mass equation:

$$\nabla(\rho \boldsymbol{u}) = S_m \tag{1}$$

Here, ρ is gas density, u is velocity vector and Sm is mass source term. Momentum equation:

$$\frac{1}{\left(\varepsilon^{eff}\right)^2}\nabla(\rho \boldsymbol{uu}) = \nabla(\mu\nabla \boldsymbol{u}) - \nabla P + S_{mom} \tag{2}$$

Here, ε^{eff} is effective porosity. μ is gas dynamic viscosity. S_{mom} is momentum source term. *P* is pressure. Species equation:

$$\nabla(\vec{u}C_k) = \nabla(D_k^{eff}\nabla C_k) + S_k \tag{3}$$

Here, C_i and D_i^{eff} are molar concentration and effective diffusivity of species *i*, respectively. Si is source term for species *i*. Charge conservation:

$$R_m + \nabla\left(\sigma_m \nabla \phi_m\right) = 0,\ R_s + \nabla\left(\sigma_s \nabla \phi_s\right) = 0 \tag{4}$$

R_m, σ_m , $\emptyset_m$ and R_s, σ_s , $\emptyset_S$, volumetric transfer current, electrical conductivity, electric potential of membrane and solid (current collector), respectively. The anode and cathode overpotentials are calculated by,

$$\eta_{anode} = \phi_s - \phi_m,\ \eta_{cathode} = \phi_s - \phi_m - V_{oc} \tag{5}$$

Here η_{anode} and $\eta_{cathode}$ are overpotential of anode and cathode. V_{oc} is open-circuit voltage. V_{oc} is 0.94 V, in this work. The operational parameters employed in the model are summarized in Table II. The boundary conditions for the model are given in Table III.

TABLE II. OPERATING PARAMETERS FOR THE MODEL

Parameter	Value
H_2 and H_2O diffusivity	7.33 x 10^{-5} m^2/s (Biyikoglu and Alpat, 2011)
O_2 diffusivity	2.13 x 10^{-5} m^2/s (Biyikoglu and Alpat, 2011)
Other species diffusivity	4.9 x 10^{-5} (Biyikoglu and Alpat, 2011)
GDL and CL porosity	0.5 (Kahveci and Taymaz, 2018)
GDL and CL viscous resistance	1 x 10^{12} $1/m^2$ (Kahveci and Taymaz, 2018)
CL surface/volume ratio	200000 1/m
Anodic reference exchange current density	4000 A/m^2
Cathodic Reference exchange current density	0.1 A/m^2

TABLE III. THE BOUNDARY CONDITIONS FOR THE MODEL

Parameter	Value
Anode and cathode inlet mass flow rates	5.398 x 10^{-6} and 3.294 x 10^{-5}kg/s
Mass fraction of H_2 and H_2O at the inlet (anode)	0.2 and 0.8
Mass fraction of O_2 and H_2O at the inlet (cathode)	0.2 and 0.1
Outlet pressure	101.325 kPa
Inlet, outlet and wall temperature at anode and cathode	343 K
Wall anode terminal (upper current collector face)	0 V
Wall cathode terminal (lower current collector face)	0-0.94 V

Volume 8, Issue 2, December 2022 - ISSN 2356-8569
http://dx.doi.org/10.21622/RESD.2022.08.2.045

The assumptions of the present computational model are: isotropic and homogenous solid (membrane, CL and GDL) materials and steady state, single phase and laminar flow.

III. RESULTS AND DISCUSSIONS

A. Validation

The numerical model used in this work was validated with experimental results from Wang et al. (2003) who used the same geometry and materials as shown in Figure 2. It is found that the developed model is reliable at lower and medium current densities since the model predictions give good agreement to the experimental data. However, at higher current densities, the overestimation of the current density is observed as a result of assuming that CL and GDL do not contain liquid water. It is found that the model used in the present work is reliable at lower and medium current densities since the model predictions demonstrate good agreement with experimental data. However, at higher current densities, the overestimation of the current density is observed as a result of assuming that CL and GDL not containing liquid water.

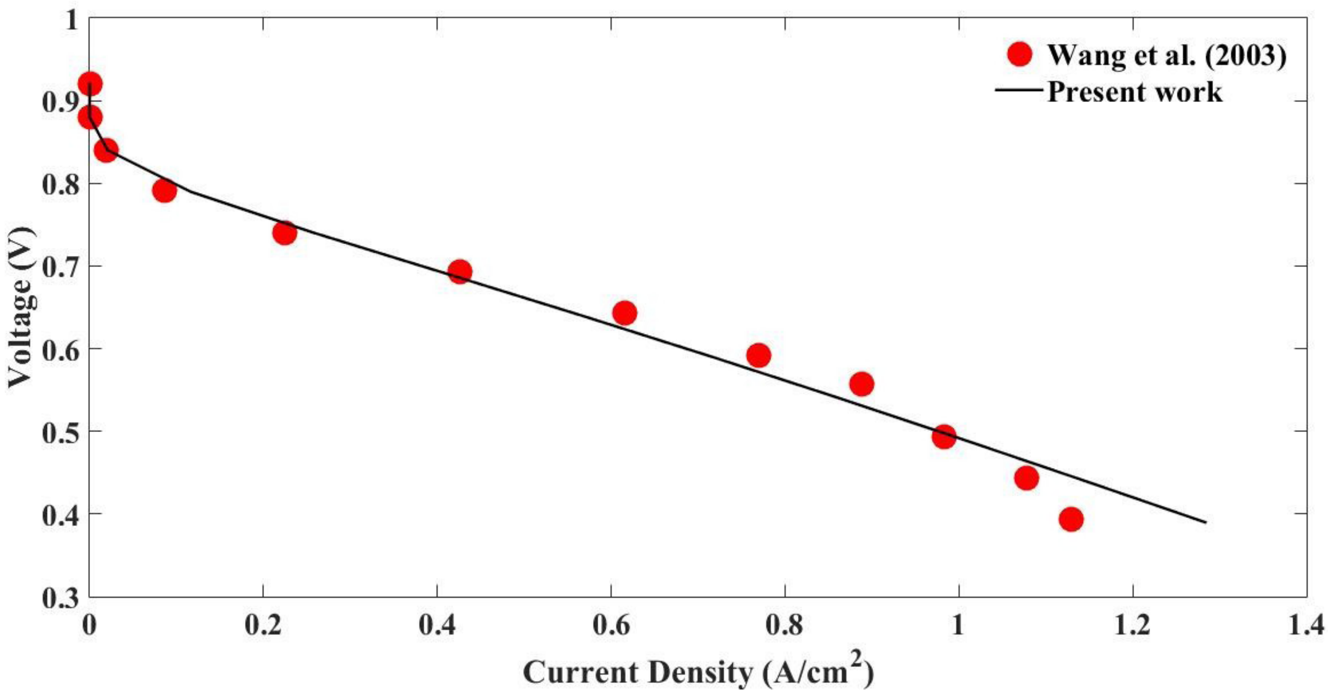

Fig. 2. Validation of the model with experimental data (Wang et al., 2003)

B. Influences of Membrane Thickness on Current Density

Figure 3 illustrates the predicted current densities for the different thicknesses of membrane varying between 0.027 and 0.189 mm at 0.4, 0.6 and 0.8 V. As displayed in Figure 3 that the current density increases nearly linearly with a decrease in the membrane thickness until 0.081 mm whereas a fast rise in the current density is examined for lower membrane thickness (<0.054 mm) at 0.4 and 0.6 V. On the other hand, almost no change in current density is observed at 0.8 V. The peak current density of 3.12 A/cm^2 is achieved with the membrane thickness of 0.027 mm. The results display that determining an optimal membrane thickness required to augment the cell efficiency.

Volume 8, Issue 2, December 2022 - ISSN 2356-8569
http://dx.doi.org/10.21622/RESD.2022.08.2.045

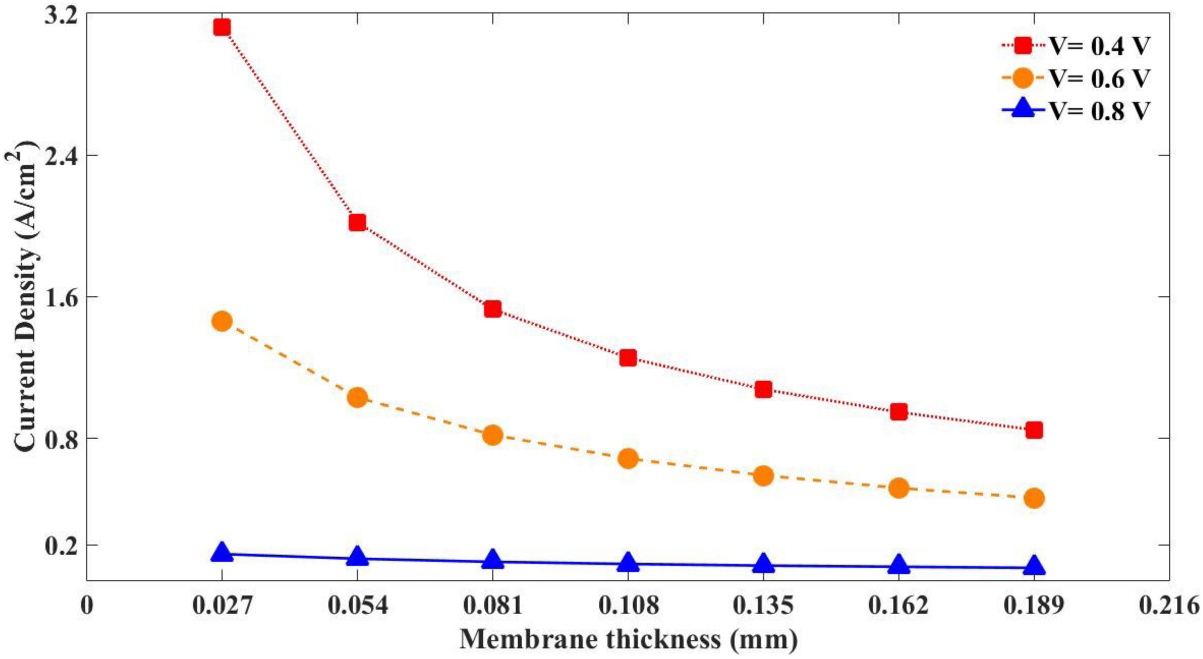

Fig. 3. Variation of current density for different membrane thicknesses at 0.4, 0.6 and 0.8 V

C. Influences of Membrane Thickness on Oxygen and Water Mass Fraction in the Cathode

In this section, since higher current density values are obtained at 4 V, the influences of membrane thicknesses on cathode oxygen and water mass fractions are examined at this cell voltage. Figures 4 illustrates the oxygen mass fraction in the plane including the membrane and cathode CL, GDL and flow channel at mid length of the cell for 0.027, 0.108 and 0.189 mm membrane thicknesses at 0.4 V.

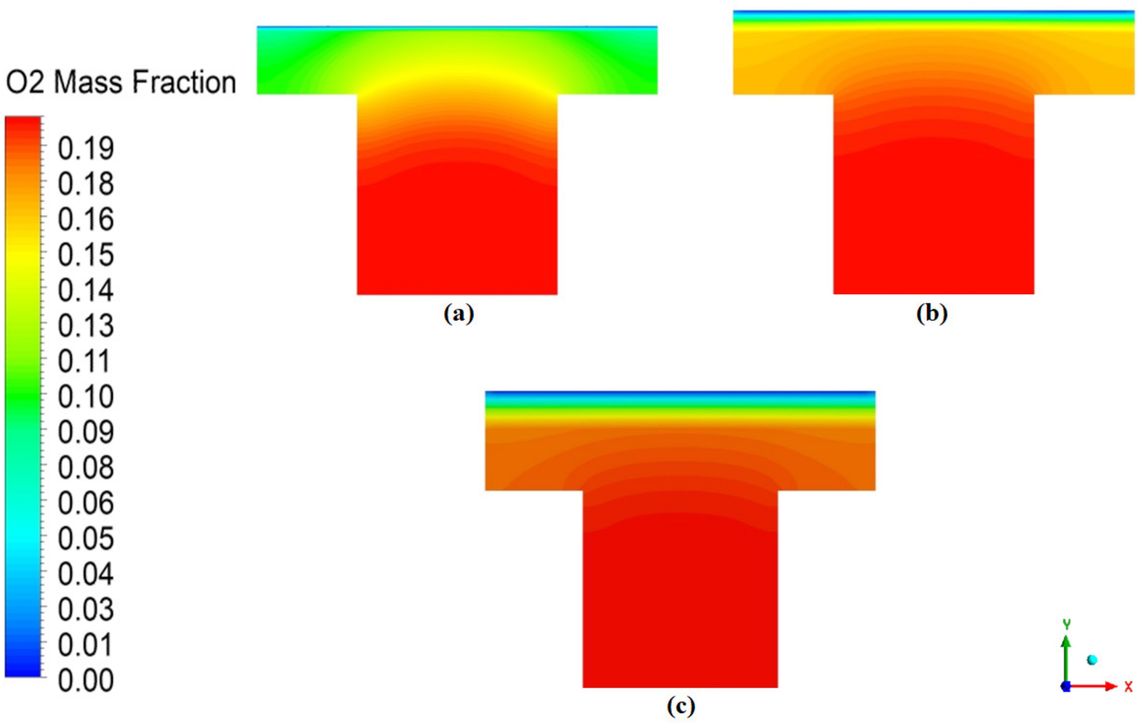

Fig. 4. Contours of O_2 mass fraction in the plane (membrane and cathode CL, GDL and flow channel) at mid length of the cell for different membrane thicknesses: (a) 0.027 mm, (b) 0.108 mm and (c) 0.189 mm (base case) at 0.4 V

http://dx.doi.org/10.21622/RESD.2022.08.2.045

It is clearly seen in Figure 4 that oxygen mass fraction in cathode GDL and CL diminishes with a decrease in membrane thickness at 0.4 V. The result proves that the cell with 0.027 mm membrane thickness generating the highest current density in Figure 3 consumes more oxygen on the cathode catalyst surface compared to other membrane thicknesses.

Figure 5 illustrates the water mass fraction in the plane including the membrane and cathode CL, GDL and flow channel at mid length of the cell for 0.027, 0.108 and 0.189 mm membrane thicknesses at 0.4 V. It is obvious in Figure 5 that decreasing membrane thickness enhances production of water during the electrochemical reaction at cathode side. Therefore, water mass fraction in cathode GDL and flow channel increases with decreasing membrane thickness as displayed in Figure 5.

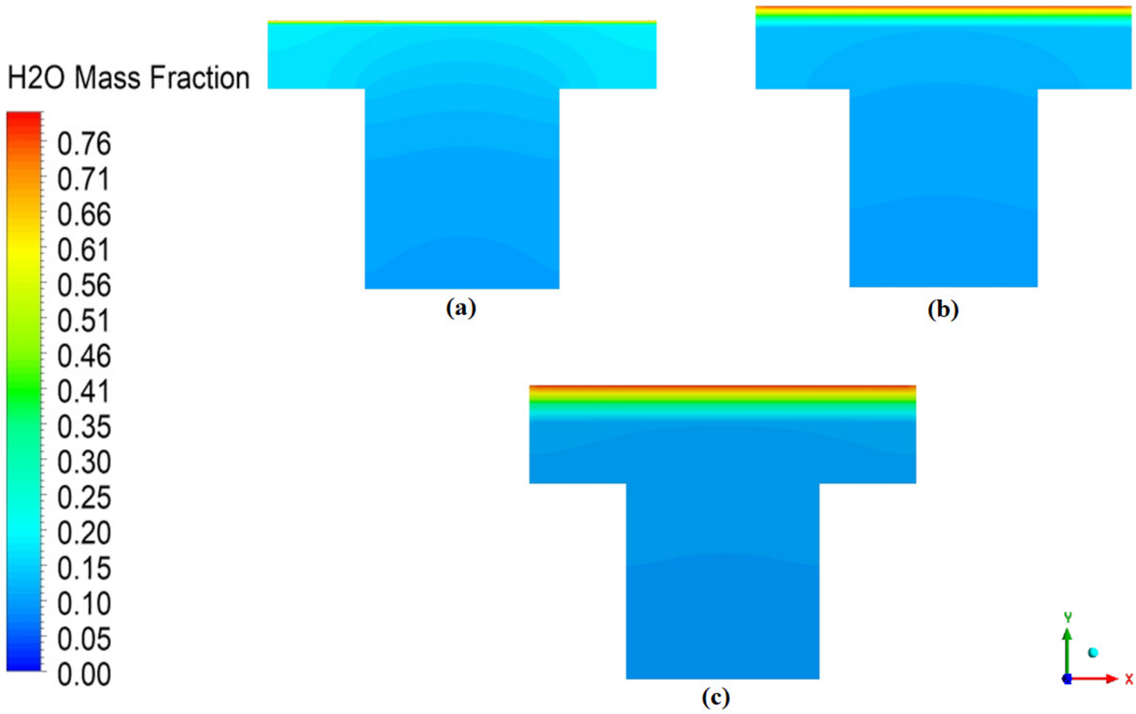

Fig. 5. Contours of H2O mass fraction in the plane (membrane and cathode CL, GDL and flow channel) at mid length of the cell for different membrane thicknesses: (a) 0.027 mm, (b) 0.108 mm and (c) 0.189 mm (base case) at 0.4 V

It is found that reducing the membrane thickness results in enhancing the cell current density associated with a higher oxygen consumption and water production and thus improves the cell performance.

D. Influences of Membrane Thickness on Pressure Drop in Anode and Cathode Channels

Table IV indicates the effects of variation of membrane thickness on pressure drop in the channels at 0.4 V.

TABLE IV. VARIATION OF PRESSURE DROP FOR DIFFERENT MEMBRANE THICKNESS

	Membrane thicknesses (mm)						
	0.027	**0.054**	**0.081**	**0.108**	**0.135**	**0.168**	**0.189**
Pressure drop (anode channel) (kPa)	0.617	0.618	0.644	0.662	0.687	0.682	0.683
Pressure drop (cathode channel) (kPa)	2.071	2.090	2.191	2.232	2.363	2.355	2.356

A large pressure drop in the flow channels leads to generate higher parasitic energy losses and increase pumping work. As shown in Table IV, pressure drop in the channels is not significantly affected by the decrease of the membrane thickness at 0.4 V. It is concluded that 0.027 mm membrane thickness provides better cell performance concerning current density and pressure drop in the channels.

http://dx.doi.org/10.21622/RESD.2022.08.2.045

IV. CONCLUSIONS

In the current study, the numerical simulation of 3-dimensional single-phase PEM fuel cell model was performed to observe the impact of different membrane thickness on the cell efficiency using the commercial ANSYS Fluent. The following are the main conclusions of the study:

1. The better PEMFC performance is achieved with the lower membrane thickness at 0.4 and 0.6 V.

2. The highest current density of 3.12 A/cm^2 is obtained with 0.027 mm membrane thickness compared with the model current density of 1.26 A/cm^2 at 0.4 V

3. A decrease in the membrane thickness results in increase oxygen consumption and water production in the cathode at 0.4 and 0.6 V.

4. No significant change in the current density is found with all membrane thicknesses at 0.8 V.

5. Variation of the membrane thickness does not have a significant impact on pressure drop in the anode and cathode channels.

6. Determining an optimal membrane thickness is needed to improve the cell efficiency.

REFERENCES

[1] ANSYS Inc., ANSYS Workbench User's Guide, Release 19.2. Canonsburg, Pennsylvania: ANSYS Inc., 2018.

[2] F. Barbir, PEM fuel cells: Theory and practice. 2012. doi: 10.1016/C2011-0-06706-6.

[3] C. Spiegel, PEM Fuel Cell Modeling and Simulation Using Matlab. 2008. doi: 10.1016/B978-0-12-374259-9.X5001-0.

[4] A. Biyikoğlu and C. Ö. Alpat, "Parametric study of a single cell proton exchange membrane fuel cell for A bundle of straight gas channels," Gazi University Journal of Science, vol. 24, no. 4, 2011.

[5] A. Iranzo, A. Salva, E. Tapia, and F. Rosa, "Effect of the membrane thermal conductivity on the performance of a polymer electrolyte membrane fuel cell," J Fuel Cell Sci Technol, vol. 11, no. 3, 2014, doi: 10.1115/1.4026522.

[6] E. E. Kahveci and I. Taymaz, "Assessment of single-serpentine PEM fuel cell model developed by computational fluid dynamics," Fuel, vol. 217, 2018, doi: 10.1016/j.fuel.2017.12.073.

[7] M. Kaplan, "Numerical investigation of influence of cross-sectional dimensions of flow channels on pem fuel cell performance," Journal of Energy Systems, vol. 5, no. 2, 2021, doi: 10.30521/jes.871018.

[8] B. Kienitz, "Optimizing polymer electrolyte membrane thickness to maximize fuel cell vehicle range," Int J Hydrogen Energy, vol. 46, no. 19, 2021, doi: 10.1016/j.ijhydene.2020.03.126.

[9] X. Luo et al., "Thickness Dependence of Proton-Exchange-Membrane Properties," J Electrochem Soc, vol. 168, no. 10, 2021, doi: 10.1149/1945-7111/ac2973.

[10] S. Mohanty, A. N. Desai, S. Singh, V. Ramadesigan, and S. M, "Effects of the membrane thickness and ionomer volume fraction on the performance of PEMFC with U-shaped serpentine channel," Int J Hydrogen Energy, vol. 46, no. 39, 2021, doi: 10.1016/j.ijhydene.2021.03.252.

[11] A. Nishimura, K. Toyoda, Y. Kojima, S. Ito, and E. Hu, "Numerical simulation on impacts of thickness of nafion series membranes and relative humidity on pemfc operated at 363 k and 373 k," Energies (Basel), vol. 14, no. 24, 2021, doi: 10.3390/en14248256.

[12] L. Xing et al., "Membrane electrode assemblies for PEM fuel cells: A review of functional graded design and optimization," Energy, vol. 177. 2019. doi: 10.1016/j.energy.2019.04.084.

[13] L. Wang, A. Husar, T. Zhou, and H. Liu, "A parametric study of PEM fuel cell performances," Int J Hydrogen Energy, vol. 28, no. 11, 2003, doi: 10.1016/S0360-3199(02)00284-7.

[14] H. W. Wu, "A review of recent development: Transport and performance modeling of PEM fuel cells," Applied Energy, vol. 165. 2016. doi: 10.1016/j.apenergy.2015.12.075.

Journal of Renewable Energy and Sustainable Development (RESD) Volume 8, Issue 2, December 2022 - ISSN 2356-8569
http://dx.doi.org/10.21622/RESD.2022.08.2.052

Received on, 02 November 2022 Accepted on, 25 November 2022 Published on, 05 December 2022

The Role of Computational Intelligence Techniques in the Advancements of Solar Photovoltaic Systems for Sustainable Development: A Review

Ranganai Tawanda Moyo[1] & Mendon Dewa[2]

[1]Department of Mechanical Engineering, Durban University of Technology, South Africa;
[2]Department of Industrial Engineering, Durban University of Technology, South Africa;

moyoranganai@gmail.com, mendond@dut.ac.za

ABSTRACT

The use of computational intelligence (CI) in solar photovoltaic (SPV) systems has been on the rise due to the increasing computational power, advancements in power electronics and the availability of data generation tools. CI techniques play an important role in modelling, sizing, forecasting, optimizing, analysing and predicting the performance and control of SPV systems. Thus, CI techniques have become an essential technology as the energy sector seeks to meet the rapidly increasing demand for clean, cheap, and reliable energy. In this context, this review paper aims to investigate the role of CI techniques in the advancements of SPV systems.

The study includes the involvement of CI techniques for parameter identification of solar cells, PV system sizing, maximum power point tracking (MPPT), forecasting, fault detection and diagnosis, inverter control and solar tracking of SPV systems. A performance comparison between CI techniques and conventional methods is also carried out to prove the importance of CI in SPV systems. The findings confirmed the superiority of CI techniques over conventional methods for every application studied and it can be concluded that the continuous improvements and involvement of these techniques can revolutionize the SPV industry and significantly increase the adoption of solar energy.

Index-words: *Solar photovoltaic systems; Computational Intelligence; Maximum power point tracking; Fault detection and diagnosis.*

I. INTRODUCTION

Sustainable development necessitates collective efforts to build an inclusive, sustainable, and resilient future for society and the planet. This means that the three pillars of sustainability; namely, economic growth, social inclusion, and environmental protection, must be balanced. It is in 2015 when the United Nations General Assembly developed seventeen Sustainable Development Goals (SDGs) as part of Agenda 2030 to ensure a sustainable future for all [1].

Fig. 1. Sustainable development goals.

 Volume 8, Issue 2, December 2022 - ISSN 2356-8569
http://dx.doi.org/10.21622/RESD.2022.08.2.052

The SDGs address all aspects of sustainability and represent an ambitious step toward actionable targets for sustainable development across all sectors of society. **Figure 1** shows the SDGs. Sustainable Development Goal 7 (SDG 7) is one of the most crucial goals and it calls for access to affordable, reliable and sustainable energy for all. Energy is a key source of economic growth in every nation and lack of access to energy supplies is a constraint to human and economic development.

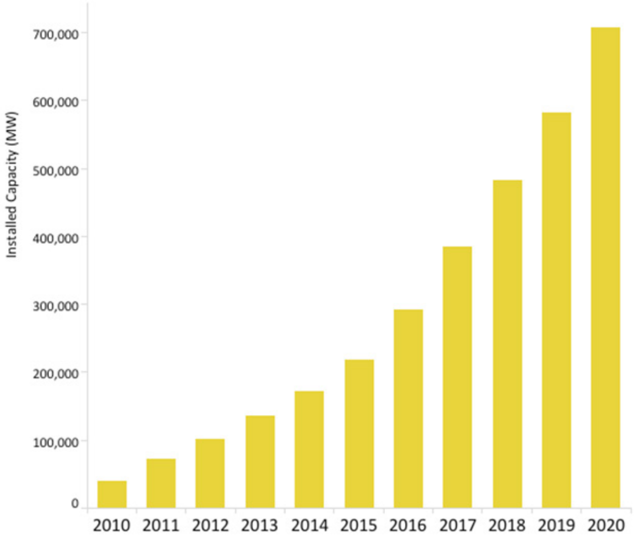

Fig. 2. Installed capacity of SPV.

Presently, fossil fuels provide approximately 80% of the world's energy [2]. The use of fossil fuels emits greenhouse gases and it is a threat to our environment. Thus, concerning SDG 7, for achieving the environmental goals for the future, many nations are strongly promoting the utilization of renewable energy sources. Renewable energy sources are sustainable and very low in pollution. In the same context, among different renewable energy sources, solar PV (SPV) is one of the fastest-growing renewable technologies as given in **Figure 2**.

The global interest in SPV is growing as the prices of photovoltaic (PV) modules and solar batteries continue to fall, as well as advances in power electronics. In addition, there are many new innovative technologies, such as computational intelligence (CI) and the internet of things (IoT), which are being used to advance SPV systems, thereby improving solar energy's competitiveness in the marketplace. CI techniques play an important role in modelling, sizing, forecasting, optimizing, analysing and predicting the performance and control of SPV systems.

They have the potential to reduce energy losses, lower energy costs, and facilitate and accelerate the global adoption of solar energy. CI techniques can also be used during the manufacturing of solar cells, allowing for the production of high-quality solar modules. Thus, CI techniques have become an essential technology as the energy sector seeks to meet the rapidly increasing demand for clean, cheap, and reliable energy.

This paper provides a comprehensive review of the application of CI techniques for modelling, sizing, optimizing, forecasting, fault detection and diagnosis, and control of SPV systems. It also gives a comparison between CI techniques and conventional methods for each application type. The rest of the paper is arranged as follows: **Section 2** gives an overview of commonly used CI techniques. **Section 3** covers the methodology and the involvement of CI techniques in different SPV systems sectors. After that, **Section 4** discusses the findings of the study and **Section 5** provides the conclusion for the study.

II. OVERVIEW OF COMMONLY USED COMPUTATIONAL INTELLIGENCE TECHNIQUES

Computational intelligence refers to the theories, designs, applications and developments of biologically and linguistically inspired computational paradigms [3]. Artificial neural networks, fuzzy systems, and evolutionary computation are the three main pillars of CI. The next section gives an outline of CI techniques.

A. Artificial Neural Networks

An artificial neural network (ANN) is a mathematical method that tries to simulate how biological neural networks work [4]. Artificial neurons learn from previous or given examples so that if they encounter such a situation again in the future, they will be able to solve it. Artificial neural networks (ANNs) have been useful in various areas including the field of medicine, neurology, mathematics, engineering, economics, and meteorology [5].

There are numerous types of ANNs, including feed-forward neural networks, recurrent networks, and radial bias neural networks. ANNs need training data sets and a learning algorithm for them to work. A commonly used learning algorithm is the back-propagation algorithm. When training ANNs, the network is given an input to give an output. The network output is then compared to the desired or correct output and if there is a difference, the synaptic weights are adjusted in such a way that decreases the error [6].

The process of adjusting the weights and running through the inputs is repeated until the errors are within the desired tolerance. After the training has reached the desired level, the weights are then held constant and the network will be ready to be used to make decisions and solve problems.

http://dx.doi.org/10.21622/RESD.2022.08.2.052

B. *Fuzzy Logic*

Lotfi Zadeh developed fuzzy logic (FL) in 1964 to address uncertainty and imprecision that are prevalent in many real-world engineering problems [7]. FL mimics decision-making in humans because it takes all possible intermediate values between "yes" and "no". Fuzzy logic is centred on the fuzzy sets theory, a theory that explains the classes of objects with ambiguous boundaries where the membership is a matter of degree [8]. A fuzzy logic controller consists of a fuzzification module, a rule-based inference system, and a defuzzification module.

The fuzzification module is responsible for transforming crisp system inputs into fuzzy values using membership functions while the inference system determines the output linguistic variables based on the fuzzy rules stored in the knowledge base. The defuzzification module then converts a linguist variable from the inference engine into a crisp output value. Fuzzy logic controllers have been utilized in different applications such as pattern recognition [9], robotics [10], aerospace [11], and many other applications.

C. *Evolutionary Computation*

Evolutionary computation is a class of population-based metaheuristic optimization algorithms that employ biological evolution-inspired mechanisms such as reproduction, mutation, recombination, and selection [12]. These evolutionary algorithms proved to be highly successful in several applications, especially for non-linear and multi-objective optimization problems. The section below gives an overview of commonly used evolutionary algorithms in PV systems.

1. Genetic Algorithms

A genetic algorithm (GA) is a search and optimization method that is devised to mimic the theory of natural selection [13]. Genetic algorithms are inspired by how living organisms adapt to the severe realities of life. A GA is implemented through three main operators namely; (a) selection operator (b) crossover operator and (c) mutation operator. When using this algorithm, the first stage is to select the initial population of genes. Then a fitness function is calculated for finding the best genes in the population.

The genes that possess the best fitness function values are selected for producing the next generation of genes using the crossover and mutation operators. The crossover operator is used to combine two chromosomes and exchange segments of their genetic material. The mutation operator is responsible for the random changes of some genes in the DNA sequence. GAs can be used for optimizing engineering designs [14], robotics [15], and many other applications. In [16], a genetic algorithm is applied for the optimum design of laminated composite structures.

2. Particle Swarm Optimization

Particle swarm optimization (PSO) is an optimization technique that is inspired by natural phenomena such as bird flocking and fish schooling [17]. Using the flocking analogy, the PSO algorithm maintains a swarm of individuals known as particles, with each particle representing a potential solution. Every particle in the swarm has a fitness value that is mapped using the objective function, and each particle also has an individual velocity that determines its motion's direction and range.

The particles share the information gleaned from their respective search processes. The position of each particle depends on two parameters: (a) the best solution obtained by a particle itself (p_{best}), and (b) the best particle in the neighbourhood (g_{best}). The particles continuously revise their direction and velocity to move towards the best position which ultimately results in each particle moving to the global optimum. PSO has been utilized for several complex applications such as water management [18], central position control in metallurgical processes [19] and robotics [20].

3. Simulated Annealing

Simulated annealing (SA) is a metaheuristic global optimization technique inspired by metallurgical annealing, in which the metal is rapidly heated to a high temperature and then slowly cooled to improve the metal's properties [21]. Using SA, the objective function represents the thermodynamic energy. At high temperatures, the algorithm allows for large movements in the search space, increasing the likelihood of accepting solutions that do not improve on the previously discovered one. This mechanism prevents the algorithm from becoming stuck in a local solution.

At low temperatures, however, the perturbation and likelihood of accepting a worse solution are greatly reduced. SA has been successfully utilized for several applications such as vehicle routing [22], farm layout optimization [23] and mechanical designs [24].

III. SOME NOVEL APPLICATIONS OF CI TECHNIQUES IN SPV SYSTEMS

A. *Methodology*

The main aim of this review paper is to provide relevant recent achievements of CI techniques in the advancements of SPV systems. Improvements in the applicability of SPV systems increase the renewable energy penetration in the world energy market

http://dx.doi.org/10.21622/RESD.2022.08.2.052

thereby reducing the use of fossil fuels and leading to sustainable development. CI techniques have been the driving force for improving the design and control of SPV systems.

To come up with a comprehensive review paper, a strict selection criterion was used. The research articles used in this work were searched from top academic research databases such as Scopus, Web of Science, IEEE Xplore and ScienceDirect. The articles are in the period, 2010 to 2022. The minimum requirement for each publication used was to have at least 10 citations. This requirement was implemented to make sure that the used material is relevant and credible.

An exception to this requirement was made for articles published in 2021 and 2022 since they did not have enough citations because of the timeframe. After meeting the minimum requirement, the articles were then selected depending on the performance of the CI techniques per given application. The performance of the CI techniques was measured using different indexes such as the root mean square error (RMSE), absolute error (AE) and efficiency (η). The papers with the best performance were then selected.

Moreover, only the papers that show a clear validation of the performance of the presented CI technique were selected. The best conventional methods per application were also included in this review paper to give a detailed comparison. The articles focused on seven different SPV system areas namely:

- Parameter identification for solar cell modelling.
- PV system sizing.
- Maximum power point tracking.
- Solar irradiance and energy production forecasting.
- Fault detection and diagnosis.
- Inverter control.
- Sun tracking.

B. Parameter Identification for Solar Cell Modelling

Accurate modelling of solar cells is a critical stage in SPV research. Due to the non-linear current-voltage characteristics of solar cells, it is very important to identify appropriate parameters for modelling the equivalent circuits of solar cells. There are two common equivalent circuits used to model solar cells; the single diode model (SD) and the double diode model (DD). The single-diode model has five parameters and the double-diode model has seven parameters. **Figure 3** shows the parameters for the single-diode model.

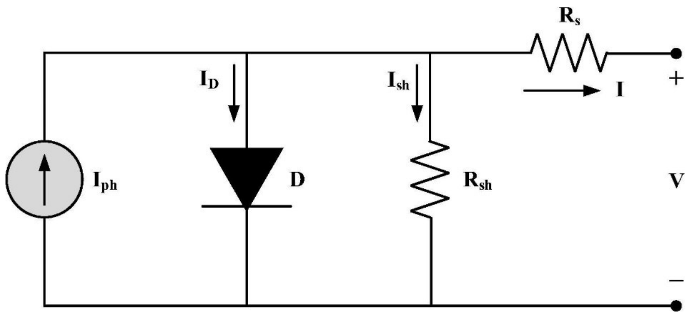

Fig. 3. An equivalent circuit for a single-diode solar cell model.

Finding the optimum values for these parameters is very crucial for modelling, controlling and sizing SPV systems. The literature presents so many methods for accurate estimation of the parameters of the solar cell and these methods can be grouped into two categories: analytical-numerical methods and CI-based methods. Analytical-numerical methods are mostly based on solving equations to determine solar cell parameters.

In [25] and [26], an analytical-numerical method was presented for solar cell parameter identification. The approach was based on curve fitting by utilizing the least square error method to form the system equations and then solving the equations using a modified Newton-Raphson (NR) method. In [27], a fast and accurate method based on the reduced forms of the original five-parameter system and experimental data was presented.

The approach was useful for a more general characterization of a PV model and only works if the experimental data sets for solar irradiance and temperatures are available. Some other analytical-numerical methods proposed for parameter identification of solar cells are given in [28, 29]. These conventional methods are easy to implement but they have many disadvantages such as the need for experimental data and relying on assumptions that can lead to the loss of accuracy when determining the solar cell equivalent circuit parameters.

CI techniques were also suggested for parameter identification of solar cell models because of their ability to solve complex and non-linear problems. In [30], genetic algorithms (GAs) were successfully applied for identifying solar cell parameters. In [31], an efficient approach based on the salp swarm algorithm (SSA) was presented for extracting the parameters of the equivalent circuit of solar cells.

The SSA was evaluated using the sine cosine algorithm, virus colony search algorithm (VCS), ant lion optimizer (ALO), gravitational search algorithm (GSA) and whale optimization algorithm (WOA). The simulation results showed that the SSA provides the highest level of accuracy and can be adopted in designing SPV systems. Other important CI techniques reported in

http://dx.doi.org/10.21622/RESD.2022.08.2.052

the literature for solving the parameter identification problem include the JAYA optimization algorithm [32], simulated annealing (SA)[33], artificial bee swarm optimization algorithm (ABSO) [34], particle swarm optimization (PSO) [35], ANN [36], and Harris hawks optimization (HHO) [37]. Hybrid techniques have also been suggested for the parameter identification of solar cells. In [38], the Levenberg-Marquardt (LM) method was combined with simulated annealing to estimate the five parameters of a single-diode model. A combination of particle swarm optimization and simulated annealing was also presented for parameter identification [39]. The performance of these methods was evaluated using the root mean square error (RMSE) given by,

$$RMSE = \sqrt{\frac{\sum_{i=1}^{N} \|y(i) - \check{y}(i)\|^{2}}{N}} \quad (1)$$

where N is the number of data points, y(i) presenting the ith measurement and $\check{y}$ (i) is its corresponding predicted value. **Table I** gives the performance of different techniques for parameter identification of solar cell models.

TABLE I: COMPARISON OF CI AND CONVENTIONAL TECHNIQUES FOR PARAMETER IDENTIFICATION OF SOLAR CELL MODELS.

Ref	Year	Author	Technique	Classification	Diode model	Performance (RMSE)
[33]	2012	K.M. El-Naggar	SA	CI	SD,DD	1.74×10^{-3}
[36]	2013	M. Karamirad	ANN	CI	SD	4.47×10^{-2}
[34]	2013	A. Askarzadeh	ABSO	CI	SD,DD	9.83×10^{-4}
[26]	2014	M. Hejri	Newton Raphson	Conventional	SD	6.35×10^{-2}
[27]	2014	A. Laudani	Reduced forms	Conventional	SD	7.73×10^{-4}
[38]	2014	F. Dkhichi	Levenberg–Marquardt &SA	CI	SD	9.86×10^{-4}
[28]	2016	M. Hejri	Approximation	Conventional	SD	2.21×10^{-2}
[32]	2017	K. Yu	JAYA	CI	SD,DD	9.83×10^{-4}
[39]	2017	M.A. Mughal	PSO-SA	CI	SD,DD	7.45×10^{-4}
[35]	2018	H.G.G. Nunes	PSO	CI	SD,DD	7.18×10^{-4}
[30]	2019	N. Hamid	GA	CI	SD,DD	2.43×10^{-3}
[25]	2020	A.K. Abdulrazzaq	Newton Raphson	Conventional	SD	1.98×10^{-6}
[31]	**2020**	**R.B. Messaoud**	**SSA**	**CI**	**SD,DD**	$\mathbf{1.30 \times 10^{-8}}$
[37]	2020	H. Chen	HHO	CI	SD,DD	6.40×10^{-4}
[29]	2021	P.J. Gnetchejo	Adaptive-Newton Raphson	Conventional	SD,DD	4.83×10^{-3}

C. PV System Sizing

Accurate sizing is one of the crucial elements to consider when designing PV systems. This includes finding the optimum number of PV modules, optimum battery storage, MPPT controllers and inverter sizes as well as the optimum placement and tilt angles of PV modules. Accurate sizing is essential because it ensures that the load demand is met and allows the design of cost-effective systems that are practically credible in the renewable energy marketplace. Analytical methods have been used for sizing PV systems. In [40], an analytical model based on the statistical analysis of the solar irradiation data was presented. The model showed satisfying results after validation. The performance of these proposed techniques was measured in terms of the correlation coefficient (r) given by,

$$r = \frac{\sum(x_i - \bar{x})(y_i - \bar{y})}{\sqrt{\sum(x_i - \bar{x})^2 . \sum(y_i - \bar{y})^2}} \quad (2)$$

where x_i represents values of the x-variable in the sample, $\bar{x}$ is the mean of the x-variable, y_i represents the values of the y-variable in the sample and $\bar{y}$ is the mean of the y-variable. In [41], the authors suggested a technique based on the Markov chain and beta probability density function for the sizing of photovoltaic generators. The obtained results were compared with the Sandia method, in which the proposed method proved to be more reliable. A model based on artificial neural networks and genetic algorithms was presented in [42] to generate the sizing curve for a stand-alone PV system. The technique was compared to the numerical methods and was considered very promising. Another technique for PV system sizing worth noting is the radial bias function neural network (RBFNN) method reported in [43]. **Table II** presents the performance of different techniques for PV system sizing.

TABLE II: COMPARISON OF CI AND CONVENTIONAL TECHNIQUES FOR PV SYSTEM SIZING.

Ref	Year	Author	Technique	Classification	Performance (r)
[41]	2010	C.V.T. Cabral	Markov chain	Conventional	0.9650
[42]	**2010**	**A. Mellit**	**ANN-GA**	**AI**	**0.9998**
[43]	2010	M. Benghanem	RBFNN	AI	0.9880
[40]	2012	E. Kaplani	Statistical analysis	Conventional	0.9500

D. *Maximum Power Point Tracking*

Maximum power point tracking (MPPT) controllers are algorithms that are included in PV battery charge controllers or inverters to extract the maximum available power from a PV module for any given temperature and irradiance [44]. For any set of temperatures and irradiance, the operating point of a PV module corresponds to a unique point on the current-voltage (I-V) curve. The operating point on the I-V curve also corresponds to some point on the power-voltage (P-V). For the PV module to produce the highest power output, its operating point must correspond to the maximum point on the P-V curve known as the Maximum Power Point (MPP) as shown in **Figure 4**.

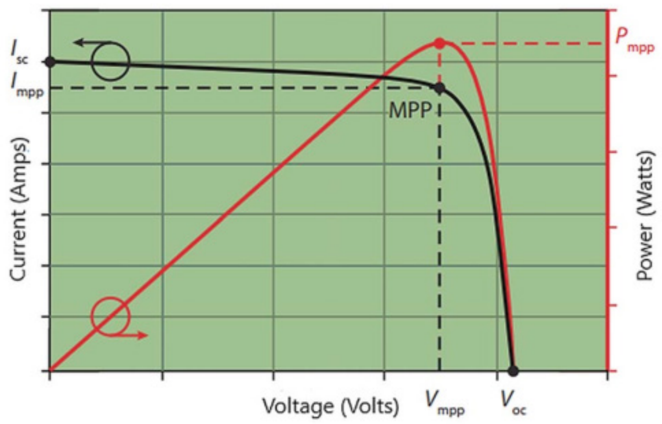

Fig. 4: I-V and P-V curves of a PV module.

If the irradiance or temperature changes, the position of the MPP also shifts. Therefore, it is the responsibility of the MPPT controller to continuously track the position of the MPPT for any given environmental condition. Generally, an MPPT controller is comprised of a DC-DC converter which is controlled by an algorithm to force the solar module's operating point to be at MPP at all times. Connecting the PV module directly to the load makes the module's operating point dictated by the load. Thus, the PV module only operates at MPP if the load impedance matches the input impedance to the DC-DC converter as seen by the PV module, otherwise it can operate at any point on the P-V curve which might not be the MPP.

MPPT techniques can be categorized as conventional techniques and CI-based techniques. The performance of the MPPT controllers was evaluated in terms of tracking efficiency calculated using the following,

$$T_{Eff} = \frac{\int_0^t P_{MPP}\, dt}{\int_0^t P_{ideal\ MPP}\, dt} \times 100\% \qquad (3)$$

where P_{MPP} represents the measured maximum power point for each controller and $P_{ideal\ MPP}$ represents the desired/ideal maximum power point for given environmental conditions. One of the widely used conventional MPPT techniques is the Perturbation and Observation (P&O) controller.

The studies [45-47] have shown how different types of the P&O method have been utilized by several researchers. Another well-known conventional technique is the incremental conductance (InCon) technique. Refs [48, 49] present the applications of different types of the InCon technique for maximum power point tracking. Some other conventional MPPT techniques include the Fractional Open-Circuit Voltage (FOCV) [50], and Fractional Short-Circuit Current (FSC) [51]. Recently, CI-based MPPT methods have been utilized and proved to be highly successful to solve the MPPT problem. In [52-54], fuzzy logic controllers were utilized for MPPT and they showed better tracking efficiency as compared to conventional techniques. Artificial neural networks were used for MPPT in Refs [55-57] and their performance was satisfactory.

Hybrid MPPT techniques were also reported in the literature where either a conventional technique is combined with a CI-based technique or combining two CI-based MPPT techniques. Examples of hybrid techniques are the GA-ANN based MPPT technique given in [58], a grey wolf–assisted perturb and observe algorithm (GWO-P&O) [59] and an adaptive neuro-fuzzy inference system (ANFIS) based technique [60]. Other CI-based MPPT techniques of interest include ANFIS-PSO-based technique [61] and genetic algorithms [62]. **Table III** presents the performance comparison of different techniques for MPPT.

TABLE III: COMPARISON OF CI AND CONVENTIONAL TECHNIQUES FOR MPPT.

Ref	Year	Author	Technique	Classification	Performance (Efficiency)
[58]	2011	R. Ramaprabha	GA-ANN	CI	99.94 %
[47]	2012	J.S. Kumari	P&O	Conventional	94.38 %
[62]	2014	S. Daraban	GA	CI	97.70 %
[53]	2014	C.L. Liu	FL	CI	99.93 %
[51]	2014	A. Sandali	FSC	Conventional	98.54 %
[49]	2015	P. Sivakumar	InCon	Conventional	96.60 %
[48]	2016	N.E. Zakzouk	InCon	Conventional	99.70 %
[50]	2016	D. Baimel	FOCV	Conventional	98.19 %
[59]	2016	S. Mohanty	GWO-P&O	CI	99.84 %
[46]	2017	V.R. Kota	P&O	Conventional	99.75 %
[54]	2017	S. Ozdemir	FL	CI	99.10 %
[45]	2018	M. Abdel-Salam	P&O	Conventional	99.48 %
[52]	2018	U. Yilmaz	FL	CI	99.40 %
[57]	2019	R. Divyasharon	ANN	CI	99.70 %
[61]	2019	N. Priyadarshi	ANFIS-PSO	CI	99.51 %
[55]	2022	S. Chahar	ANN	CI	96.48 %
[56]	2022	S.R. Kiran	ANN	CI	98.15 %
[60]	**2022**	**R.T. Moyo**	**ANFIS**	**CI**	**99.97 %**

E. Forecasting

Forecasting in SPV systems can be grouped into two types named: (a) solar irradiance forecasting and (b) forecasting of energy production. Solar irradiance forecasting involves the estimation of the irradiance expected to be received over a certain period. Energy production forecasting focuses on the estimation of the power output from the PV modules. The forecast information is very crucial for the management and control of solar PV hybrids systems as well as for energy trading [63]. Several methods of different architecture and complexity have been explored to solve this forecasting problem. Forecasting in SPV systems can also be grouped as short-term, mid-term or long-term forecasting and different forecasting methodologies have been utilized depending on the type of problem. The performance of the techniques in this category was evaluated using the RMSE given by Equation (1).

 Volume 8, Issue 2, December 2022 - ISSN 2356-8569
http://dx.doi.org/10.21622/RESD.2022.08.2.052

1. Irradiance Forecasting

Forecasting solar irradiance is essential for grid-connected photovoltaic (PV) plant performance and power estimation. Both conventional and modern techniques have been used for irradiance forecasting. In [64], the authors presented a statistical Fourier trend model for short-term solar irradiance forecasting. Their model was able to achieve around 90% forecasting accuracy and produced better results as compared to other popular statistical models. In [65], an automated convolutional neural network long short-term memory (CNN-LSTM) architecture was designed for forecasting solar irradiance.

The proposed model outperformed other models in terms of the MAE, RMSE and Pearson metrics. Other techniques that show better results as applied to solar irradiance forecasting include deep recurrent neural networks (DRNNs) [66] and convolutional neural networks. Table IV shows a review of different techniques as applied to solar irradiance forecasting as well as their performances.

TABLE IV: COMPARISON OF CI AND CONVENTIONAL TECHNIQUES FOR SOLAR IRRADIANCE FORECASTING.

Ref	Year	Author	Technique	Classification	Performance (RMSE)
[64]	2013	Z. Dong	Statistical Fourier trend model	Conventional	0.1964
[66]	2017	A. Alzahrani	DRNNs	C1	0.0860
[67]	2019	S. Ghimire	Convolutional neural networks	CI	0.1801
[65]	**2021**	**S.M.J. Jalali**	**CNN-LSTM**	**CI**	**0.0136**

2. Forecasting of the Power Production

The power generated by photovoltaic modules is affected by solar irradiation and temperature. As a result, predicting the output power is a hot topic for photovoltaic experts to research. The literature reports different kinds of methods to tackle this problem. In [68], a seasonal decomposition least-square support vector regression model was proposed to forecast monthly solar power output.

After a comparative study, it was found that the ESDLS-SVR model performed better as compared to other statistical models such as the autoregressive integrated moving average (ARIMA) and seasonal autoregressive integrated moving average (SARIMA).

Another method was presented in [69], to forecast a day-ahead power output from PV plants based on the least-square optimization technique. To validate the model, the methodology was compared with previous studies and the results were promising.

An ANN-based model was also used to forecast the average power output from PV modules [70]. In this model, GAs were utilized to optimize the parameters of the ANN architecture. The findings showed that the proposed model performs better than other forecasting models such as ARIMA.

Other important techniques that have been used for forecasting the output power of PV modules include the variation auto-encoder-driven deep learning approach [71] and gated recurrent unit recurrent neural networks (GRU-RNN) [72]. **Table V** shows the performance of different techniques for energy production forecasting.

Volume 8, Issue 2, December 2022 - ISSN 2356-8569
http://dx.doi.org/10.21622/RESD.2022.08.2.052

TABLE V: COMPARISON OF CI AND CONVENTIONAL TECHNIQUES FOR ENERGY PRODUCTION FORECASTING.

Ref	Year	Author	Technique	Classification	Performance (RMSE)
[70]	2012	H.T.C. Pedro	ANN-GA model	CI	0.1307
[68]	2016	K.P. Lin	ESDLS-SVR	Conventional	0.1618
[69]	2016	D.P. Larson	Least-squares optimization model	Conventional	0.1020
[71]	2020	A. Dairi	Deep learning	CI	0.1731
[72]	**2021**	**A.A. Du Plessis**	**GRU-RNN**	**CI**	**0.0802**

F. Fault Detection and Diagnosis

PV systems typically operate in harsh outdoor environments. The PV system is prone to different types of system faults and defects when operating in such a setting. These faults and defects can come from the PV array itself or the components connected to it. PV array-related faults can be grouped into three categories depending on their time characteristics. **Figure 5** shows PV array-related faults. Other faults that come from components connected to the PV arrays include MPPT faults and inverter faults.

Numerous fault detection and diagnosis techniques have been developed and suggested to identify the type and location of different failures in a PV system. The main idea is to develop a robust technique that can detect evolving faults quickly to increase the system's reliability and lifetime. Fault detection methods listed in the literature include visual methods, imaging techniques, electrical methods and computational intelligence techniques. For this application, the techniques were evaluated using the prediction efficiency given by,

$$\eta = \frac{P_c}{N} \times 100\% \qquad (4)$$

where P_c is the number of correct predictions made and N is the total number of test examples. In [73], a fault and diagnosis procedure based on the probabilistic neural networks (PNN) was presented. The proposed technique demonstrated a higher efficiency as compared to the feed-forward back-propagation artificial neural networks for noiseless and noisy data.

An enhanced ensemble learning technique was utilized in [74] to detect and diagnose the faults in a grid-connected PV system. The testing results of this technique indicated a high prediction accuracy of 99.96 %. In [75], a technique based on supervised machine learning was presented.

The technique was tested using real grid-connected PV data and the results showed the effectiveness of the proposed method. A statistical technique based on the univariate and multivariate exponentially weighted moving average (EWMA) was also used for fault detection of PV systems [76].

This technique was implemented using real data and the results proved its capabilities in detecting partial shading. Some other fault detection techniques worth noting are the decision tree algorithm [77], laterally primed adaptive resonance theory (LAPART) [78], regression-based approach [79], machine learning (k-nearest neighbours) [80], fine-tuning naive bayesian model [81] and ANFIS [82]. **Table IV** presents the performance analysis of different techniques for fault detection and diagnosis.

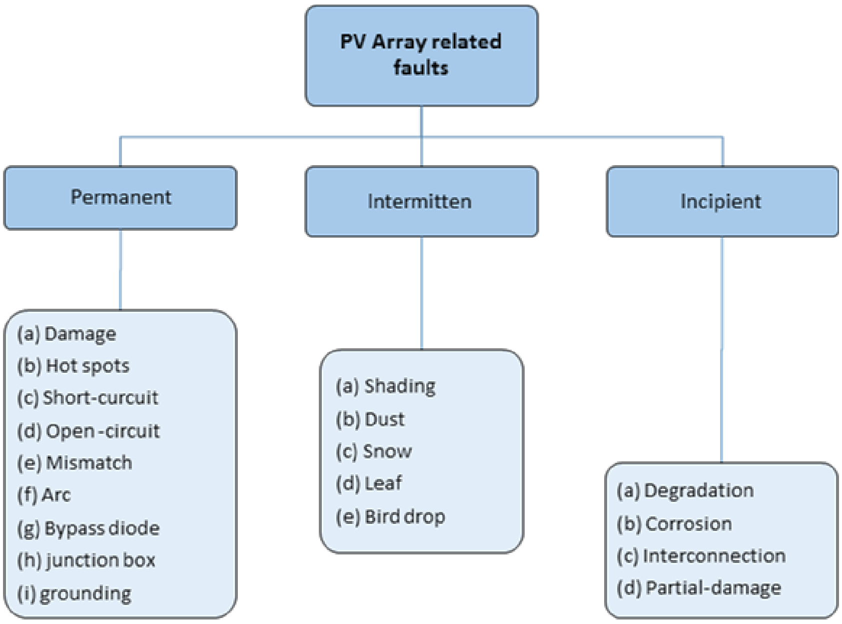

Fig. 5. PV array-related faults.

TABLE VI: COMPARISON OF CI AND CONVENTIONAL TECHNIQUES FOR FAULT DETECTION AND DIAGNOSIS.

Ref	Year	Author	Technique	Classification	Performance (Efficiency)
[78]	2015	C.B. Jones	LAPART	Conventional	86.00 %
[73]	2017	E. Garoudja	PNN	CI	98.09 %
[77]	2018	R. Benkercha	Decision tree algorithm	CI	99.80 %
[82]	2018	M. Dhimish	ANFIS	CI	92.10 %
[80]	2018	S.R. Madeti	Machine learning	CI	98.70 %
[76]	2018	F. Harrou	EWMA	Conventional	95.00 %
[79]	2019	A. Dhoke	Regression-based approach	Conventional	97.00 %
[75]	2021	M. Hajji	Machine learning	CI	99.03 %
[74]	**2021**	**K. Dhibi**	**Enhanced ensemble learning**	**CI**	**99.96 %**
[81]	2021	W. He	Fine-Tuning Naive Bayesian Model	Conventional	98.59 %

G. Inverter Control

In PV systems, there exist DC/AC inverters responsible for generating the 3-phase AC voltage for the load. The main aim of inverter control is to regulate the AC output voltage and frequency to make sure that it has low harmonic distortions. This is to make sure that the power that is being supplied to the load is of good quality. Different techniques have been developed and suggested for inverter control of PV systems. The performance of the proposed techniques in this section was evaluated using total harmonic distortion (THD) given by,

$$THD_{(v)}(\%) = \frac{1}{V_1}\sqrt{\sum_{h=2}^{\infty} V_h^2} \times 100 \quad (5)$$

where V_1 is the fundamental voltage and V_h represents the h^{th} harmonic voltage. In [83], the authors proposed a multilevel inverter for SPV systems based on fuzzy logic control. The proposed system showed improved performance as compared to two-level inverters and under low to medium power range. In [84], a technique based on the IoT and ANN was proposed for monitoring and controlling a SPV system. The proposed method was simulated in MATLAB/Simulink environment and the results were compared to the proportional-integral (PI) controller.

The results showed that the proposed technique was efficient and able to monitor the THD, voltages and phase angle variations within the required limits. In [85], a 3-phase three-level inverter was designed and implemented for controlling the current and voltage of a SPV system. The control was realized using a PI controller. The performance of this technique was satisfying and it can also be applied for very high powers. A quasi-Z-source inverter was also suggested for inverter control of SPV systems [86]. The developed topology was implemented using a proportional-integral sinusoidal (PIS) controller. In [87], an adaptive sliding mode (SM) control was utilized for a two-level inverter to control a grid-connected SPV system.

The proposed technique showed better results as compared to other schemes at different load and solar irradiance levels. Some other inverter control techniques worth noting include the adaptive neuro-fuzzy inference system and proportional-integral-derivative control (ANFIS-PID) [88], pulse-width-modulation (PWM) control scheme [89] and vector control (VC) [90]. **Table VII** shows the performance of different techniques for inverter control.

TABLE VII: COMPARISON OF CI AND CONVENTIONAL TECHNIQUES FOR INVERTER CONTROL.

Ref	Year	Author	Technique	Classification	Performance (THD)
[83]	2010	C. Cecati	FL	CI	3.10 %
[86]	2010	M .Shahparasti	PIS	Conventional	3.62 %
[89]	2010	N.A. Rahim	PWM	Conventional	3.90 %
[85]	2014	S. Ozdemir	PI	Conventional	3.45 %
[87]	2015	N. Kumar	SM	Conventional	4.75 %
[88]	2017	N. Mahmud	ANFIS-PID	CI	2.70 %
[90]	2019	N. Kumar	VC	Conventional	2.96 %
[84]	**2020**	**J. Gupta**	**IoT-ANN**	**CI**	**2.61 %**

H. Solar Tracking System

Solar tracking systems are controllers used to guide PV modules towards the sun. They improve the efficiency of PV modules by making sure that the modules are always aligned with the rotating sun. It was proven that solar trackers increase the power output of solar panels up to 60% more than a stationery system [91].

There are mainly two types of solar trackers; single-axis and dual-axis tracking controllers. Different mechanisms have been developed and proposed for solar tracking. The performance of these techniques is measured in terms of the increase in power output (IPO) as compared to a stationary system.

$$IPO(\%) = \left(\frac{P_T - P_F}{P_F}\right) \times 100 \quad (6)$$

where P_T is the power generated by the studied tracking system and P_F is the power from a fixed flat-plate system. In [92], a dual-axis programmable logical controller (PLC) was designed and implemented for solar tracking. The controller was compared with

http://dx.doi.org/10.21622/RESD.2022.08.2.052

a fixed-angle PV system and the results confirmed the superiority of the proposed method. In [93], an ultraviolet (UV) sensor-based dual-axis solar tracking system was presented. For validation, the proposed technique was compared to a fixed-angle system and a light-depended resistors (LDRs) based solar tracking system. The results showed that the proposed technique is reliable and profitable. An FL controller is suggested for the design of a dual-axis solar tracking system as reported in [94]. This controller was fully automatic and it was able to consider the changes in weather patterns. In [95], a technique based on DELTA PLC was proposed. The tracking was performed with the help of LDR sensors and magnetic reed switches to control the direction and the speed of the gear motor. The power generation from the proposed system showed a significant increase as compared to that obtained from a fixed system. **Table VIII** presents the performance of different techniques for solar tracking.

TABLE VIII: COMPARISON OF CI AND CONVENTIONAL TECHNIQUES FOR SOLAR TRACKING SYSTEMS.

Ref	Year	Author	Technique	Classification	Performance (IPO)
[92]	2013	T.S. Zhan	PLC	Conventional	25.00 %
[94]	**2016**	**C.H. Huang**	**FL**	**CI**	**36.00 %**
[95]	2016	B.K.S. Vastav,	DELTA PLC	Conventional	25.00 %
[93]	2021	C. Jamroen	UV	Conventional	19.97 %

IV. DISCUSSION

In this paper, more than 300 articles were reviewed. The main emphasis was to provide relevant achievements of CI techniques in SPV systems. The paper gives a comparison of different CI techniques as well as conventional methods in each application in terms of their performance. This section provides the findings of the study.

Parameter identification of solar cell models is very crucial since it is the backbone for SPV modelling and design. Several techniques of different complexities were proposed to tackle this problem. Generally, the CI techniques showed better performances as compared to conventional methods with the SSA achieving the RMSE of 1.30×10^{-8} for both the SD and DD models. Other CI techniques that performed well for both the SD and DD models are the GA, JAYA algorithm, PSO and SA.

The best conventional method was the Newton-Raphson technique with the RMSE of 1.98×10^{-6}. However, this technique was only tested for a SD model. A conventional method which was tested for both the SD and DD models is the Adaptive-Newton Raphson and it performed fairly with a RMSE of 4.83×10^{-3}. It can be concluded that CI techniques have significantly improved the parameter estimation of solar cell models and it is very vital for the accurate modelling of SPV systems.

Accurate sizing of the components of a SPV system is very important when designing solar systems. Over-sizing of SPV systems would lead to unnecessary higher investments whereas under-sizing may cause an insufficient power supply to connected loads. Both conventional and CI techniques were utilized for sizing SPV systems. The performance of these techniques was measured using the correlation coefficient. A CI technique based on ANN and GAs was found to be the best with a correlation coefficient of 0.9998 followed by the RBFNN method. The best conventional method was the Markov chain technique which showed a correlation coefficient of 0.9650. For this application, it can be concluded that the involvement of CI has improved the sizing of SPV systems.

Maximum power point tracking controllers play a pivotal role in maximizing the power output of solar modules. In general, a MPPT controller is a DC-DC power converter controlled by an algorithm to always force the PV module to operate at its MPP. The best of both the conventional and CI techniques were reviewed and they all showed an outstanding performance for MPPT. The best technique was a CI-based method (ANFIS) with an efficiency of 99.97%. A GA-ANN method also gave an outstanding performance with an efficiency of 99.94%. Some other CI techniques that performed well for this application are FL, ANFIS-PSO and GWO-P&O. Conventional techniques also showed an impressive performance with the best technique (P&O) with an efficiency of 99.75%. The incremental conductance was the second-best conventional technique with an efficiency of 99.70%. From the above-presented analysis, it is clear that CI techniques have been instrumental in designing MPPT controllers.

Forecasting in SPV systems involves solar irradiance forecasting and energy production forecasting. Solar irradiance forecasting focuses on estimating the irradiance to be received at a particular place and time whereas energy production forecasting deals with predicting the power output from PV modules.

Generally, it was observed that forecasting is very difficult when it comes to SPV systems and it was deduced from high RMSE values in both cases. However, CI techniques performed better than conventional methods and the automated CNN-LSTM was the best technique for irradiance forecasting with a RMSE of 0.0136. A conventional technique that showed better results for irradiance forecasting was the statistical Fourier trend model with a RMSE of 0.1964. For energy production forecasting, the GRU-RNN was found to be the best with a RMSE of 0.0802. The least-squares optimization model was the conventional technique with better results for energy production forecasting with a RMSE of 0.1020. It can be then concluded that CI techniques have improved both irradiance forecasting and energy production forecasting of SPV systems.

Fault detection and diagnosis techniques are very important to ensure the maximum performance of SPV systems. Several methods were developed and suggested for fault detection and diagnosis. CI techniques proved to be more efficient in this application as compared to conventional methods. A technique based on enhanced ensemble learning was found to be the best with an efficiency of 99.96%. Other CI techniques that performed well include decision tree algorithm, PNN and different machine learning techniques. A conventional method that performed fairly was the Fine-Tuning Naïve Bayesian model, with an efficiency of 98.59%. Based on the given analysis, it can be concluded that the adoption of CI techniques for fault detection and diagnosis has a greater impact on the development of SPV systems.

In PV systems, inverters are used to transform DC to AC for the loads. Inverter control involves regulating the output AC voltage and frequency to ensure the supply of power of good quality to the loads. In this application, both the conventional and CI techniques demonstrated outstanding performance for inverter control. The best technique was the IoT-ANN, a CI technique, with a maximum THD of 2.61%. An ANFIS-PID method was the second best with a THD of 2.70%. Conventional techniques proved their relevance for this application with their best technique with a THD of 2.96%. For this application, CI techniques were the best, but conventional methods were also competing in the same range.

Solar tracking systems are important for ensuring that the PV modules are always aligned with the rotating sun. All techniques presented for this application performed well. The FL controller was the best technique with an IPO of 36% and it was the only CI technique in this application. Conventional methods that showed better performance were the PLC and DELTA PLC, both with an IPO of 25%. It can be concluded that CI techniques have shown an improvement as far as solar tracking is concerned but there is still room for the adoption of more CI for solving this particular problem.

V. CONCLUSIONS

This paper explores the role of CI techniques in the advancements of SPV systems for sustainable development. The conclusion that can be drawn from this work is that CI techniques are involved in every aspect of SPV systems and have significantly improved the adoption of SPV systems. This paper compares different CI techniques and conventional methods in terms of performance. In all SPV areas studied, CI techniques proved to be superior to conventional methods. In the literature, several CI techniques have been developed and suggested for different applications, however, selecting an appropriate technique for a given application is of prime importance. Thus, the findings from this work can assist other researchers to choose suitable CI techniques for a given application. This paper also serves as a reference for all academics interested in studying the application of computational intelligence in SPV systems.

REFERENCES

[1] A. Fleming, R. M. Wise, H. Hansen, and L. Sams, "The sustainable development goals: A case study," Marine Policy, vol. 86, pp. 94-103, December 2017, doi: 10.1016/j.marpol.2017.09.019.

[2] A. Hassan, S. Z. Ilyas, A. Jalil, and Z. Ullah, “Monetization of the environmental damage caused by fossil fuels,” Environmental Science and Pollution Research, vol. 28, no. 17, 2021, doi: 10.1007/s11356-020-12205-w.

[3] V. Sugumaran, T. v. Geetha, D. Manjula, and H. Gopal, “Guest Editorial: Computational Intelligence and Applications,” Information Systems Frontiers, vol. 19, no. 5. 2017. doi: 10.1007/s10796-017-9794-7.

[4] L. Vanneschi and M. Castelli, "Multilayer Perceptrons," in Encyclopedia of Bioinformatics and Computational Biology, S. Ranganathan, M. Gribskov, K. Nakai, and C. Schönbach Eds. Oxford: Academic Press, 2019, pp. 612-620.

[5] S. A. Kalogirou, "Artificial neural networks in energy applications in buildings," International Journal of Low-Carbon Technologies, vol. 1, issue 3, pp. 201-216, July 2006, doi: 10.1093/ijlct/1.3.201.

[6] T. P. Lillicrap, D. Cownden, D. B. Tweed, and C. J. Akerman, "Random synaptic feedback weights support error backpropagation for deep learning," Nat Commun, vol. 7, 2016, doi: 10.1038/ncomms13276.

[7] E. M. Sharma, "A Survey in fuzzy Logic: An Introduction," in The National Seminar on Recent Advanced in wireless Networks and Communication (NWNC), Ajmer, India, 2014.

[8] M. Kochen, "APPLICATIONS OF FUZZY SETS IN PSYCHOLOGY," in Fuzzy Sets and their Applications to Cognitive and Decision Processes, L. A. Zadeh, K.-S. Fu, K. Tanaka, and M. Shimura Eds. California: Academic Press, 1975, pp. 395-408.

[9] A. Zardecki, "Fuzzy control for forecasting and pattern recognition in a time series," in IEEE International Conference on Fuzzy Systems, 1994, vol. 3. doi: 10.1109/fuzzy.1994.343584.

[10] S. X. Yang, H. Li, M. Q. H. Meng, and P. X. Liu, "An embedded fuzzy controller for a behavior-based mobile robot with guaranteed performance," IEEE Transactions on Fuzzy Systems, vol. 12, no. 4, 2004, doi: 10.1109/TFUZZ.2004.832524.

[11] O. Castillo, L. Cervantes, J. Soria, M. Sanchez, and J. R. Castro, "A generalized type-2 fuzzy granular approach with applications to aerospace," Inf Sci (N Y), vol. 354, 2016, doi: 10.1016/j.ins.2016.03.001.

[12] Kaveh, P. Rahmani, and A. D. Eslamlou, "An efficient hybrid approach based on Harris Hawks optimization and imperialist competitive algorithm for structural optimization," Eng Comput, vol. 38, 2022, doi: 10.1007/s00366-020-01258-7.

[13] M. Mijwil, "Genetic Algorithm Optimization by Natural Selection," Masters, Department of Computer Scince, Baghdad University, Baghdad, Iraq, 2016.

[14] L. G. Caldas and L. K. Norford, "A design optimization tool based on a genetic algorithm," Automation in construction, vol. 11, issue 2, pp. 173-184, February 2002, doi: 10.1016/S0926-5805(00)00096-0

[15] L. Tian and C. Collins, "An effective robot trajectory planning method using a genetic algorithm," Mechatronics, vol. 14, no. 5, 2004, doi: 10.1016/j.mechatronics.2003.10.001.

[16] P. Y. Tabakov and S. Moyo, "A comparative analysis of evolutionary algorithms in the design of laminated composite structures," Science and Engineering of Composite Materials, vol. 24, no. 1, 2017, doi: 10.1515/secm-2014-0385.

[17] U. A. Salaria, M. I. Menhas, and S. Manzoor, "Quasi oppositional population based global particle swarm optimizer with inertial weights (qpgpso-w) for solving economic load dispatch problem," IEEE Access, vol. 9, 2021, doi: 10.1109/ACCESS.2021.3116066.

[18] M. Jahandideh-Tehrani, O. Bozorg-Haddad, and H. A. Loáiciga, "Application of particle swarm optimization to water management: an introduction and overview," Environmental Monitoring and Assessment, vol. 192, no. 5. 2020. doi: 10.1007/s10661-020-8228-z.

[19] L. Jia and X. Zhao, "An Improved Particle Swarm Optimization (PSO) Optimized Integral Separation PID and its Application on Central Position Control System," IEEE Sens J, vol. 19, no. 16, 2019, doi: 10.1109/JSEN.2019.2912849.

[20] G. Rossides, B. Metcalfe, and A. Hunter, "Particle swarm optimization-an adaptation for the control of robotic swarms," Robotics, vol. 10, no. 2, 2021, doi: 10.3390/robotics10020058.

[21] B. Morales-Castañeda, D. Zaldívar, E. Cuevas, O. Maciel-Castillo, I. Aranguren, and F. Fausto, "An improved Simulated Annealing algorithm based on ancient metallurgy techniques," Applied Soft Computing Journal, vol. 84, 2019, doi: 10.1016/j.asoc.2019.105761.

[22] B. Rabbouch, F. Saâdaoui, and R. Mraihi, "Empirical-type simulated annealing for solving the capacitated vehicle routing problem," Journal of Experimental and Theoretical Artificial Intelligence, vol. 32, no. 3, 2020, doi: 10.1080/0952813X.2019.1652356.

[23] K. Yang and K. Cho, "Simulated annealing algorithm for wind farm layout optimization: A benchmark study," Energies (Basel), vol. 12, no. 23, 2019, doi: 10.3390/en12234403.

[24] M. Abd Elaziz, A. H. Elsheikh, D. Oliva, L. Abualigah, S. Lu, and A. A. Ewees, "Advanced Metaheuristic Techniques for Mechanical Design Problems: Review," Archives of Computational Methods in Engineering, vol. 29, no. 1, 2022, doi: 10.1007/s11831-021-09589-4.

[25] A. K. Abdulrazzaq, G. Bognár, and B. Plesz, "Accurate method for PV solar cells and modules parameters extraction using I–V curves," Journal of King Saud University - Engineering Sciences, July 2020, doi: https://doi.org/10.1016/j.

jksues.2020.07.008.

[26] M. Hejri, H. Mokhtari, M. R. Azizian, M. Ghandhari, and L. Söder, "On the parameter extraction of a five-parameter double-diode model of photovoltaic cells and modules," IEEE J Photovolt, vol. 4, no. 3, 2014, doi: 10.1109/JPHOTOV.2014.2307161.

[27] Laudani, F. Riganti Fulginei, and A. Salvini, "High performing extraction procedure for the one-diode model of a photovoltaic panel from experimental I-V curves by using reduced forms," Solar Energy, vol. 103, 2014, doi: 10.1016/j.solener.2014.02.014.

[28] M. Hejri, H. Mokhtari, M. R. Azizian, and L. Söder, "An analytical-numerical approach for parameter determination of a five-parameter single-diode model of photovoltaic cells and modules," International Journal of Sustainable Energy, vol. 35, no. 4, 2016, doi: 10.1080/14786451.2013.863886.

[29] P. J. Gnetchejo et al., "A Self-adaptive Algorithm with Newton Raphson Method for Parameters Identification of Photovoltaic Modules and Array," Transactions on Electrical and Electronic Materials, vol. 22, no. 6, 2021, doi: 10.1007/s42341-021-00312-5.

[30] N. Hamid, R. Abounacer, M. Idali Oumhand, M. Feddaoui, and D. Agliz, "Parameters identification of photovoltaic solar cells and module using the genetic algorithm with convex combination crossover," International Journal of Ambient Energy, vol. 40, no. 5, 2019, doi: 10.1080/01430750.2017.1421577.

[31] R. ben Messaoud, "Extraction of uncertain parameters of single and double diode model of a photovoltaic panel using Salp Swarm algorithm," Measurement (Lond), vol. 154, 2020, doi: 10.1016/j.measurement.2019.107446.

[32] K. Yu, J. J. Liang, B. Y. Qu, X. Chen, and H. Wang, "Parameters identification of photovoltaic models using an improved JAYA optimization algorithm," Energy Convers Manag, vol. 150, 2017, doi: 10.1016/j.enconman.2017.08.063.

[33] K. M. El-Naggar, M. R. AlRashidi, M. F. AlHajri, and A. K. Al-Othman, "Simulated Annealing algorithm for photovoltaic parameters identification," Solar Energy, vol. 86, no. 1, 2012, doi: 10.1016/j.solener.2011.09.032.

[34] Askarzadeh and A. Rezazadeh, "Artificial bee swarm optimization algorithm for parameters identification of solar cell models," Appl Energy, vol. 102, 2013, doi: 10.1016/j.apenergy.2012.09.052.

[35] H. G. G. Nunes, J. A. N. Pombo, S. J. P. S. Mariano, M. R. A. Calado, and J. A. M. Felippe de Souza, "A new high performance method for determining the parameters of PV cells and modules based on guaranteed convergence particle swarm optimization," Appl Energy, vol. 211, 2018, doi: 10.1016/j.apenergy.2017.11.078.

[36] M. Karamirad, M. Omid, R. Alimardani, H. Mousazadeh, and S. N. Heidari, "ANN based simulation and experimental verification of analytical four- and five-parameters models of PV modules," Simul Model Pract Theory, vol. 34, 2013, doi: 10.1016/j.simpat.2013.02.001.

[37] H. Chen, S. Jiao, M. Wang, A. A. Heidari, and X. Zhao, "Parameters identification of photovoltaic cells and modules using diversification-enriched Harris hawks optimization with chaotic drifts," J Clean Prod, vol. 244, 2020, doi: 10.1016/j.jclepro.2019.118778.

[38] F. Dkhichi, B. Oukarfi, A. Fakkar, and N. Belbounaguia, "Parameter identification of solar cell model using Levenberg-Marquardt algorithm combined with simulated annealing," Solar Energy, vol. 110, 2014, doi: 10.1016/j.solener.2014.09.033.

[39] M. A. Mughal, Q. Ma, and C. Xiao, "Photovoltaic cell parameter estimation using hybrid particle swarm optimization and simulated annealing," Energies (Basel), vol. 10, no. 8, 2017, doi: 10.3390/en10081213.

[40] E. Kaplani and S. Kaplanis, "A stochastic simulation model for reliable PV system sizing providing for solar radiation fluctuations," Appl Energy, vol. 97, 2012, doi: 10.1016/j.apenergy.2011.12.016.

[41] C. V. T. Cabral, D. O. Filho, A. S. A. C. Diniz, J. H. Martins, O. M. Toledo, and L. de V. B. Machado Neto, "A stochastic method for stand-alone photovoltaic system sizing," Solar Energy, vol. 84, no. 9, 2010, doi: 10.1016/j.solener.2010.06.006.

[42] Mellit, S. A. Kalogirou, and M. Drif, "Application of neural networks and genetic algorithms for sizing of photovoltaic systems," Renew Energy, vol. 35, no. 12, 2010, doi: 10.1016/j.renene.2010.04.017.

[43] M. Benghanem and A. Mellit, "Radial Basis Function Network-based prediction of global solar radiation data: Application for sizing of a stand-alone photovoltaic system at Al-Madinah,

Saudi Arabia," Energy, vol. 35, no. 9, 2010, doi: 10.1016/j.energy.2010.05.024.

[44] S. Salman, X. Ai, and Z. Wu, "Design of a P-&-O algorithm based MPPT charge controller for a stand-alone 200W PV system," Protection and Control of Modern Power Systems, vol. 3, no. 1, 2018, doi: 10.1186/s41601-018-0099-8.

[45] M. Abdel-Salam, M. T. El-Mohandes, and M. Goda, "An improved perturb-and-observe based MPPT method for PV systems under varying irradiation levels," Solar Energy, vol. 171, 2018, doi: 10.1016/j.solener.2018.06.080.

[46] V. R. Kota and M. N. Bhukya, "A novel linear tangents based P&O scheme for MPPT of a PV system," Renewable and Sustainable Energy Reviews, vol. 71. 2017. doi: 10.1016/j.rser.2016.12.054.

[47] J. S. Kumari, D. C. S. Babu, and A. K. Babu, "Design and analysis of P&O and IP&O MPPT techniques for photovoltaic system," International Journal of Modern Engineering Research, vol. 2, no. 4, 2012.

[48] N. E. Zakzouk, M. A. Elsaharty, A. K. Abdelsalam, A. A. Helal, and B. W. Williams, "Improved performance low-cost incremental conductance PV MPPT technique," IET Renewable Power Generation, vol. 10, no. 4, 2016, doi: 10.1049/iet-rpg.2015.0203.

[49] P. Sivakumar, A. Abdul Kader, Y. Kaliavaradhan, and M. Arutchelvi, "Analysis and enhancement of PV efficiency with incremental conductance MPPT technique under non-linear loading conditions," Renew Energy, vol. 81, 2015, doi: 10.1016/j.renene.2015.03.062.

[50] D. Baimel, R. Shkoury, L. Elbaz, S. Tapuchi, and N. Baimel, "Novel optimized method for maximum power point tracking in PV systems using Fractional Open Circuit Voltage technique," in 2016 International Symposium on Power Electronics, Electrical Drives, Automation and Motion, SPEEDAM 2016, 2016. doi: 10.1109/SPEEDAM.2016.7525984.

[51] Sandali, T. Oukhoya, and A. Cheriti, "Modeling and design of PV grid connected system using a modified fractional short-circuit current MPPT," in Proceedings of 2014 International Renewable and Sustainable Energy Conference, IRSEC 2014, 2014. doi: 10.1109/IRSEC.2014.7059859.

[52] U. Yilmaz, A. Kircay, and S. Borekci, "PV system fuzzy logic MPPT method and PI control as a charge controller," Renewable and Sustainable Energy Reviews, vol. 81. 2018. doi: 10.1016/j.rser.2017.08.048.

[53] C. L. Liu, J. H. Chen, Y. H. Liu, and Z. Z. Yang, "An asymmetrical fuzzy-logic-control-based MPPT algorithm for photovoltaic systems," Energies (Basel), vol. 7, no. 4, 2014, doi: 10.3390/en7042177.

[54] S. Ozdemir, N. Altin, and I. Sefa, "Fuzzy logic based MPPT controller for high conversion ratio quadratic boost converter," Int J Hydrogen Energy, vol. 42, no. 28, 2017, doi: 10.1016/j.ijhydene.2017.02.191.

[55] S. Chahar and D. Yadav, "Performance Analysis of Soft Computing ANN Based MPPT Technique for Solar PV Generator," in 2022 IEEE World Conference on Applied Intelligence and Computing (AIC), Sonbhadra, India, 2022: IEEE, pp. 98-102.

[56] S. R. Kiran, C. H. Basha, V. P. Singh, C. Dhanamjayulu, B. R. Prusty, and B. Khan, "Reduced Simulative Performance Analysis of Variable Step Size ANN Based MPPT Techniques for Partially Shaded Solar PV Systems," IEEE Access, vol. 10, issue 1, pp. 48875-48889, 2022, doi: 10.1109/ACCESS.2022.3172322.

[57] R. Divyasharon, R. Narmatha Banu, and D. Devaraj, "Artificial Neural Network based MPPT with CUK Converter Topology for PV Systems under Varying Climatic Conditions," in IEEE International Conference on Intelligent Techniques in Control, Optimization and Signal Processing, INCOS 2019, 2019. doi: 10.1109/INCOS45849.2019.8951321.

[58] R. Ramaprabha, V. Gothandaraman, K. Kanimozhi, R. Divya, and B. L. Mathur, "Maximum power point tracking using GA-optimized artificial neural network for solar PV system," in 2011 1st International Conference on Electrical Energy Systems, ICEES 2011, 2011. doi: 10.1109/ICEES.2011.5725340.

[59] S. Mohanty, B. Subudhi, and P. K. Ray, "A grey wolf-assisted perturb & observe MPPT algorithm for a PV system," IEEE Transactions on Energy Conversion, vol. 32, issue. 1, pp. 340-347, December 2016, doi: 10.1109/TEC.2016.2633722.

[60] R. T. Moyo, P. Y. Tabakov, and S. Moyo, "Comparative analysis of different computational intelligence techniques for maximum power point tracking of PV systems," Journal of Sustainable Energy, vol. 13, issue 1, pp. 12-22, June 2022, doi: 10.5281/ZENODO.7139169.

[61] N. Priyadarshi, S. Padmanaban, J. B. Holm-Nielsen, F. Blaabjerg, and M. S. Bhaskar, "An Experimental Estimation of Hybrid ANFIS-PSO-Based MPPT for PV Grid Integration under Fluctuating Sun Irradiance," IEEE Syst J, vol. 14, no. 1, 2020, doi: 10.1109/JSYST.2019.2949083.

[62] S. Daraban, D. Petreus, and C. Morel, "A novel MPPT (maximum power point tracking) algorithm based on a modified genetic algorithm specialized on tracking the global maximum power point in photovoltaic systems affected by partial shading," Energy, vol. 74, no. C, 2014, doi: 10.1016/j.energy.2014.07.001.

[63] Bugała et al., "Short-term forecast of generation of electric energy in photovoltaic systems," Renewable and Sustainable Energy Reviews, vol. 81. 2018. doi: 10.1016/j.rser.2017.07.032.

[64] Z. Dong, D. Yang, T. Reindl, and W. M. Walsh, "Short-term solar irradiance forecasting using exponential smoothing state space model," Energy, vol. 55, 2013, doi: 10.1016/j.energy.2013.04.027.

[65] S. M. J. Jalali, S. Ahmadian, A. Kavousi-Fard, A. Khosravi, and S. Nahavandi, "Automated Deep CNN-LSTM Architecture Design for Solar Irradiance Forecasting," IEEE Trans Syst Man Cybern Syst, vol. 52, no. 1, 2022, doi: 10.1109/TSMC.2021.3093519.

[66] Alzahrani, P. Shamsi, C. Dagli, and M. Ferdowsi, "Solar Irradiance Forecasting Using Deep Neural Networks," in Procedia Computer Science, 2017, vol. 114. doi: 10.1016/j.procs.2017.09.045.

[67] S. Ghimire, R. C. Deo, N. Raj, and J. Mi, "Deep solar radiation forecasting with convolutional neural network and long short-term memory network algorithms," Appl Energy, vol. 253, 2019, doi: 10.1016/j.apenergy.2019.113541.

[68] K. P. Lin and P. F. Pai, "Solar power output forecasting using evolutionary seasonal decomposition least-square support vector regression," J Clean Prod, vol. 134, no. Part B, 2016, doi: 10.1016/j.jclepro.2015.08.099.

[69] D. P. Larson, L. Nonnenmacher, and C. F. M. Coimbra, "Day-ahead forecasting of solar power output from photovoltaic plants in the American Southwest," Renew Energy, vol. 91, 2016, doi: 10.1016/j.renene.2016.01.039.

[70] H. T. C. Pedro and C. F. M. Coimbra, "Assessment of forecasting techniques for solar power production with no exogenous inputs," Solar Energy, vol. 86, no. 7, 2012, doi: 10.1016/j.solener.2012.04.004.

[71] Dairi, F. Harrou, Y. Sun, and S. Khadraoui, "Short-term forecasting of photovoltaic solar power production using variational auto-encoder driven deep learning approach," Applied Sciences (Switzerland), vol. 10, no. 23, 2020, doi: 10.3390/app10238400.

[72] A. A. du Plessis, J. M. Strauss, and A. J. Rix, "Short-term solar power forecasting: Investigating the ability of deep learning models to capture low-level utility-scale Photovoltaic system behaviour," Appl Energy, vol. 285, 2021, doi: 10.1016/j.apenergy.2020.116395.

[73] E. Garoudja, A. Chouder, K. Kara, and S. Silvestre, "An enhanced machine learning based approach for failures detection and diagnosis of PV systems," Energy Convers Manag, vol. 151, 2017, doi: 10.1016/j.enconman.2017.09.019.

[74] K. Dhibi, M. Mansouri, K. Bouzrara, H. Nounou, and M. Nounou, "An Enhanced Ensemble Learning-Based Fault Detection and Diagnosis for Grid-Connected PV Systems," IEEE Access, vol. 9, 2021, doi: 10.1109/ACCESS.2021.3128749.

[75] M. Hajji et al., "Multivariate feature extraction based supervised machine learning for fault detection and diagnosis in photovoltaic systems," Eur J Control, vol. 59, 2021, doi: 10.1016/j.ejcon.2020.03.004.

[76] F. Harrou, Y. Sun, B. Taghezouit, A. Saidi, and M. E. Hamlati, "Reliable fault detection and diagnosis of photovoltaic systems based on statistical monitoring approaches," Renew Energy, vol. 116, 2018, doi: 10.1016/j.renene.2017.09.048.

[77] R. Benkercha and S. Moulahoum, "Fault detection and diagnosis based on C4. 5 decision tree algorithm for grid connected PV system," Solar Energy, vol. 173, issue 1, pp. 610-634, October 2018, doi: 10.1016/j.solener.2018.07.089.

[78] C. B. Jones, J. S. Stein, S. Gonzalez, and B. H. King, "Photovoltaic system fault detection and diagnostics using Laterally Primed Adaptive Resonance Theory neural network," in 2015 IEEE 42nd Photovoltaic Specialist Conference, PVSC 2015, 2015. doi: 10.1109/PVSC.2015.7355834.

[79] Dhoke, R. Sharma, and T. K. Saha, "An approach for fault detection and location in solar PV systems," Solar Energy, vol. 194, 2019, doi: 10.1016/j.solener.2019.10.052.

http://dx.doi.org/10.21622/RESD.2022.08.2.052

[80] S. R. Madeti and S. N. Singh, "Modeling of PV system based on experimental data for fault detection using kNN method," Solar Energy, vol. 173, 2018, doi: 10.1016/j.solener.2018.07.038.

[81] W. He, D. Yin, K. Zhang, X. Zhang, and J. Zheng, "Fault detection and diagnosis method of distributed photovoltaic array based on fine-tuning naive bayesian model," Energies (Basel), vol. 14, no. 14, 2021, doi: 10.3390/en14144140.

[82] M. Dhimish, V. Holmes, B. Mehrdadi, and M. Dales, "Comparing Mamdani Sugeno fuzzy logic and RBF ANN network for PV fault detection," Renew Energy, vol. 117, 2018, doi: 10.1016/j.renene.2017.10.066.

[83] C. Cecati, F. Ciancetta, and P. Siano, "A multilevel inverter for photovoltaic systems with fuzzy logic control," IEEE Transactions on Industrial Electronics, vol. 57, no. 12, 2010, doi: 10.1109/TIE.2010.2044119.

[84] J. Gupta, M. K. Singla, P. Nijhawan, S. Ganguli, and S. S. Rajest, "An IoT-Based Controller Realization for PV System Monitoring and Control," in EAI/Springer Innovations in Communication and Computing, 2020. doi: 10.1007/978-3-030-44407-5_13.

[85] S. Ozdemir, N. Altin, and I. Sefa, "Single stage three level grid interactive MPPT inverter for PV systems," Energy Convers Manag, vol. 80, 2014, doi: 10.1016/j.enconman.2014.01.048.

[86] M. Shahparasti, A. Sadeghi Larijani, A. Fatemi, A. Yazdian Varjani, and M. Mohammadian, "Quasi Z-source inverter for photovoltaic system connected to single phase AC grid," in PEDSTC 2010 - 1st Power Electronics and Drive Systems and Technologies Conference, 2010. doi: 10.1109/PEDSTC.2010.5471773.

[87] N. Kumar, T. K. Saha, and J. Dey, "Sliding-Mode Control of PWM Dual Inverter-Based Grid-Connected PV System: Modeling and Performance Analysis," IEEE J Emerg Sel Top Power Electron, vol. 4, no. 2, 2016, doi: 10.1109/JESTPE.2015.2497900.

[88] N. Mahmud, A. Zahedi, and A. Mahmud, "A Cooperative Operation of Novel PV Inverter Control Scheme and Storage Energy Management System Based on ANFIS for Voltage Regulation of Grid-Tied PV System," IEEE Trans Industr Inform, vol. 13, no. 5, 2017, doi: 10.1109/TII.2017.2651111.

[89] N. A. Rahim, K. Chaniago, and J. Selvaraj, "Single-phase seven-level grid-connected inverter for photovoltaic system," IEEE Transactions on Industrial Electronics, vol. 58, no. 6, 2011, doi: 10.1109/TIE.2010.2064278.

[90] N. Kumar, T. K. Saha, and J. Dey, "Multilevel Inverter (MLI)-Based Stand-Alone Photovoltaic System: Modeling, Analysis, and Control," IEEE Syst J, vol. 14, no. 1, 2020, doi: 10.1109/JSYST.2019.2900485.

[91] M. T. A. Khan, S. M. S. Tanzil, R. Rahman, and S. M. S. Alam, "Design and construction of an automatic solar tracking system," in ICECE 2010 - 6th International Conference on Electrical and Computer Engineering, 2010. doi: 10.1109/ICELCE.2010.5700694.

[92] T. S. Zhan, W. M. Lin, M. H. Tsai, and G. S. Wang, "Design and implementation of the dual-axis solar tracking system," in Proceedings - International Computer Software and Applications Conference, 2013. doi: 10.1109/COMPSAC.2013.46.

[93] C. Jamroen, C. Fongkerd, W. Krongpha, P. Komkum, A. Pirayawaraporn, and N. Chindakham, "A novel UV sensor-based dual-axis solar tracking system: Implementation and performance analysis," Appl Energy, vol. 299, 2021, doi: 10.1016/j.apenergy.2021.117295.

[94] C. H. Huang, H. Y. Pan, and K. C. Lin, "Development of intelligent fuzzy controller for a two-axis solar tracking system," Applied Sciences, vol. 6, no. 5, 2016, doi: 10.3390/app6050130.

[95] B. K. S. Vastav, S. Nema, P. Swarnkar, and D. Rajesh, "Automatic solar tracking system using DELTA PLC," in International Conference on Electrical Power and Energy Systems, ICEPES 2016, 2017. doi: 10.1109/ICEPES.2016.7915899.

http://apc.aast.edu

مركز الأكاديمية للنشر
ACADEMY Publishing Center

Renewable Energy and Sustainable Development Journal

Volume 8, Issue 2, December 2022 - ISSN 2356-8569